THE ASTROPHYSICAL JOURNAL, 492:521–539, 1998 January 10

PHYSICAL CONDITIONS OF THE MOLECULAR GAS IN SEYFERT GALAXIES

PADELI P. PAPADOPOULOS AND E. R. SEAQUIST
Department of Astronomy, University of Toronto, 60 St. George Street, Toronto, Ontario M5S 3H8, Canada
Received 1997 February 24; accepted 1997 August 22

ABSTRACT

We examine the physical conditions of the global molecular gas reservoir in the host galaxies of Seyfert 1 and Seyfert 2 nuclei. To do so, we acquired sensitive ^{12}CO, ^{13}CO, $J = 1$–0, and $J = 2$–1 observations and collected available data from the literature for a sample of 27 Seyfert galaxies. We find that Seyfert galaxies have an average value for the ^{12}CO/^{13}CO $J = 1$–0 and $J = 2$–1 line ratios of $\langle R_{10} \rangle = 12$ and $\langle R_{21} \rangle = 13$, respectively, with no discernible dependence on the Seyfert type.

The $r_{12} = (2\text{–}1)/(1\text{–}0)$ line ratio for ^{12}CO does not reveal any significant difference between the two types, but Seyfert galaxies as a class seem to have systematically lower values of r_{12} (~ 0.5–0.7) than do average spirals and starbursts. Moreover, for all the galaxies examined, but especially for Seyfert and starburst galaxies, we find that r_{12} is likely to be smaller as the area of the galaxy sampled by the telescope beam becomes larger. This may be the consequence of a global gas excitation gradient in galaxies where warm ($T_{\rm kin} \gtrsim 20$ K) gas lies confined, preferably in their central regions ($\lesssim 1$ kpc), while a colder ($T_{\rm kin} \lesssim 10$ K), and possibly subthermally excited, gas phase dominates the more extended CO emission in the disk. For Seyfert and starburst galaxies, there are indications that their gas excitation gradients may be quite similar.

Examination of the properties of the molecular gas by using the r_{12}, R_{10}, and R_{21} line ratios reveals that, unless $r_{12} \lesssim 0.6$, a single warm gas phase can account for the observed values of these ratios toward the central regions of an average Seyfert and/or starburst galaxy.

Subject headings: galaxies: ISM — galaxies: Seyfert — galaxies: starburst — radio lines: galaxies

1. INTRODUCTION

An important aspect of the Seyfert phenomenon is the possible relationship between the properties of the host galaxy (e.g., star formation rate) and the presence of the active galactic nucleus (AGN) (e.g., Norman & Scoville 1988; Heckman et al. 1989; Linden et al. 1993). The cause is thought to be infalling molecular gas that acts as a "fuel" for both the star formation and the AGN. The difference between the two types of Seyfert galaxies is thought to arise because of a dense molecular gas torus with a size of $L \sim 1$–10 pc (Krolik & Begelman 1986) that obscures the AGN in Seyfert 2 (hereafter Sy2) galaxies but not in Seyfert 1 (hereafter Sy1) galaxies. The small size of this torus makes any direct dependence of its characteristics on global ($L \gtrsim 1$ kpc) properties of the host galaxy (e.g., molecular gas mass and star formation rate) rather unlikely.

Nevertheless, Heckman et al. (1989) find that Sy2 galaxies have on average ~ 4 times higher far-infrared luminosity than Sy1 or non-Seyfert galaxies. They also find that Sy2 galaxies have higher CO luminosity than Sy1 or non-Seyfert galaxies when normalized to other global variables like the blue luminosity or the H I content of the host galaxy. These results imply that Sy2 galaxies have higher star formation rates and are more gas rich than Sy1 and similar field galaxies over scales of $L \gtrsim 1$ kpc. Later studies (Maiolino et al. 1995, 1997) that use a larger sample do not confirm the "excess" CO luminosity of Sy2 galaxies, but they do find that Sy2 galaxies are undergoing starbursts more often than Sy1 galaxies. Such results cannot be reconciled easily with a small size for the AGN-obscuring torus and point toward a more complex picture where the obscuring material may be distributed on much larger scales than previously thought (Maiolino & Rieke 1995).

Many studies examining the molecular gas of starburst galaxies have shown that the gas excitation is significantly higher in the circumnuclear star-forming region than in quiescent regions in the galactic disk or similar regions in the Milky Way (e.g., Rieke et al. 1980; Wall et al. 1993; Devereux et al. 1994; Aalto et al. 1995). This is to be expected since elevated star formation with the associated high density of O and B stars and the high supernova rate heats, disrupts, and compresses molecular clouds. Therefore, it is possible that the global gas excitation properties of the two Seyfert types are different, with type 2 containing, on average, warmer molecular gas than type 1. Furthermore, since the majority of Seyfert galaxies are of type 2 (Maiolino & Rieke 1995), a corollary is that Seyfert galaxies as a class have elevated star formation rates compared with similar field galaxies. Further evidence that starbursts may play an important role in the Seyfert phenomenon can also be found in studies of the featureless UV continuum (Heckman et al. 1995) observed in these galaxies, where a circumnuclear starburst as well as the AGN (e.g., Barvainis 1993) may be contributing to the UV luminosity.

For these reasons, we used millimeter spectroscopy of the ^{12}CO, ^{13}CO $J = 1$–0, 2–1 lines in order to probe the global gas excitation properties in Seyfert galaxies and to examine whether elevated star formation rates have any discernible effect on them. Extensive data sets found in the literature for the ^{12}CO (2–1)/(1–0) ratio in starburst, LINER, and quiescent galaxies allowed us to extend our study to other classes of galaxies with different types and degrees of nuclear activity, and to compare them with the Seyfert galaxies in our sample. Throughout this study, we assume $H_0 = 75$ km s^{-1} Mpc^{-1} and $q_0 = 0.5$.

2. OBSERVATIONS AND DATA REDUCTION

2.1. *Sample Selection*

Our sample includes almost all (24) the Seyfert galaxies in the Heckman et al. (1989) survey that have been detected in

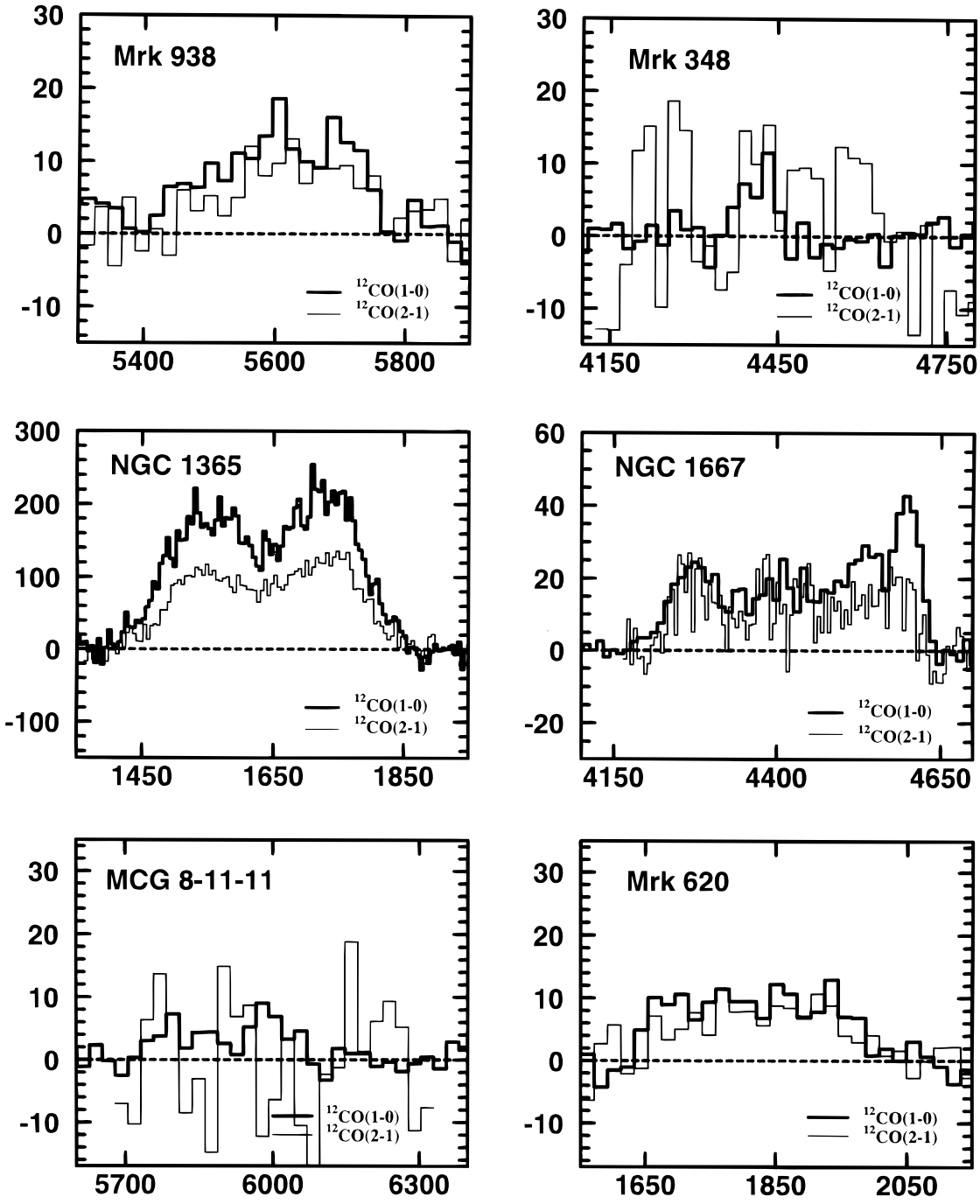

FIG. 1.—The ^{12}CO, $J = 2$–1, $J = 1$–0 spectra observed with the NRAO 12 m telescope (except NGC 7172 and Ark 564). The velocity is in units of km s^{-1} (Heliocentric). The temperature is in units of millikelvin, and the temperature scale is T_{mb}.

the ^{12}CO $J = 1$–0 transition, plus the Sy1 galaxy Ark 564 and the LINER (previously classified as a Sy2 galaxy) NGC 6764, both of which were not included in the Heckman et al. sample. In the literature, we found multitransition CO data with reliable estimates of line ratios for two more Sy1 galaxies, namely, I Zw 1 and Mrk 817, which we include in our study. Note that these objects have been classified previously as radio-quiet quasars (RQQs), but several studies (Morgan & Dreiser 1983; Chini, Kreysa, & Biermann 1989; Alloin et al. 1992) indicate that RQQs are simply Sy1 galaxies seen at a greater distance.

2.2. *NRAO* 12 m *Observations*

We used the NRAO 12 m telescope[1] in two four-day observing runs starting on 1994 April 28 and 1995 April 19 to observe the ^{12}CO $J = 1$–0, 2–1 transitions at 115 and 230 GHz, respectively, for all the galaxies in the sample, and ^{13}CO $J = 1$–0 at 110 GHz in all cases where reasonably strong ^{12}CO emission was detected. The profile of the tele-

[1] The National Radio Astronomy Observatory (NRAO) is a facility of the NSF, operated under a cooperative agreement by Associated Universities, Inc.

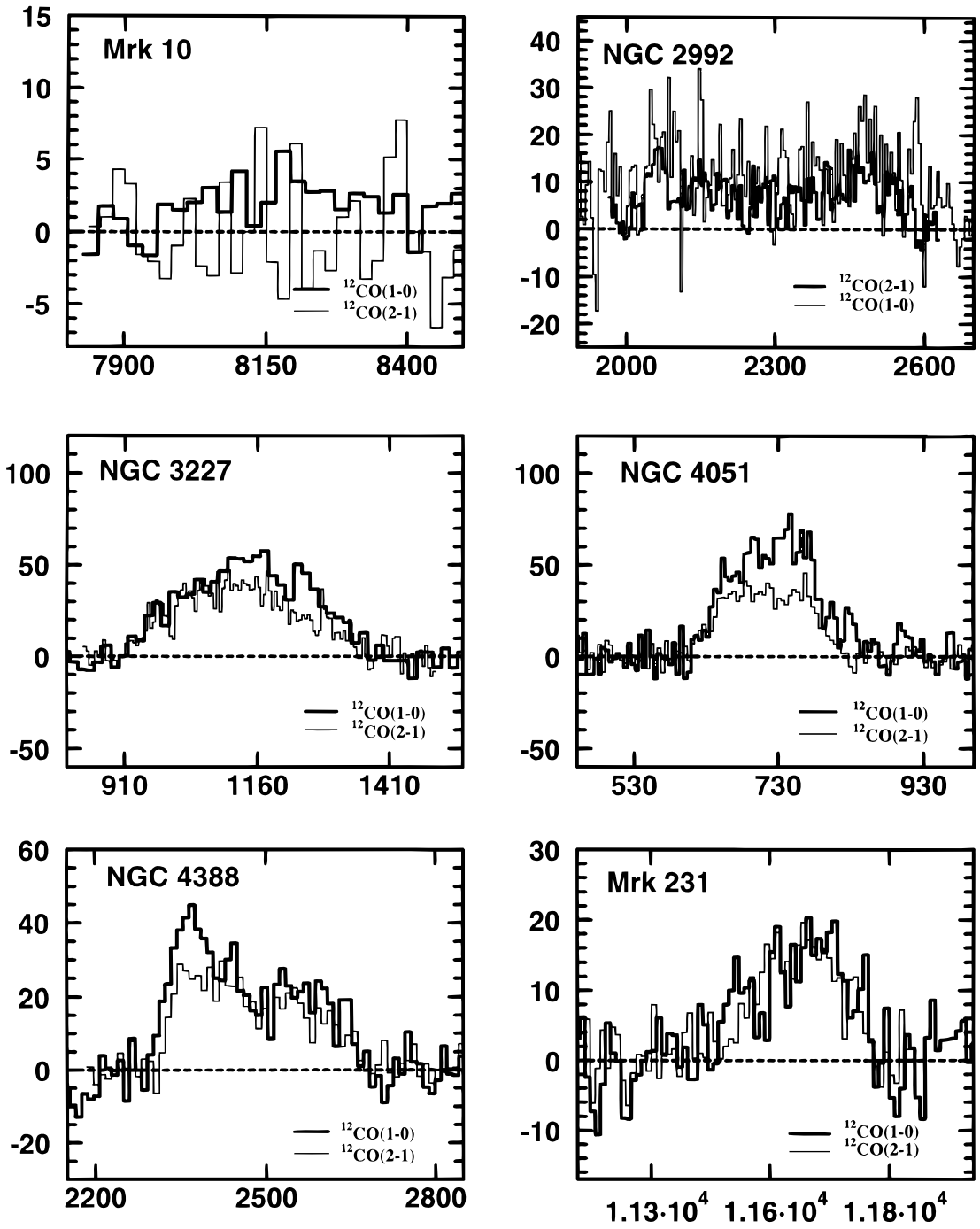

FIG. 1—*Continued*

scope main beam is closely approximated by a Gaussian with a half-power beamwidth (HPBW) of 55″ and 32″ at 115 and 230 GHz, respectively. We monitored the focus and pointing of the telescope by frequently observing bright quasars and planets. The rms pointing error was found to be ~7″ in both frequencies. We performed all observations using a beam-switching mode with beam throws 4′–6′ in azimuth, and at rates of 1.25–2.5 Hz. The 256 × 2 MHz filter bank was used, giving a velocity range of 1336 km s^{-1} at 115 GHz and 668 km s^{-1} at 230 GHz. We have converted the original temperature scale T_R^* of the NRAO 12 m spectra to the T_{mb} scale, assuming efficiencies of n_M^* (115 GHz) = 0.80 and n_M^* (230 GHz) = 0.48 (Jewell 1990).

Spectral-line observations of small-diameter standard sources were performed with and without beam switching in order to search for any systematic effects during the nutation of the secondary. No such effects were found for the beam throws and frequencies employed during our observing runs. The rapid beam-switching mode gave us remarkably flat baselines in most of our spectra. As a result, only linear baselines had to be removed.

A principal goal is to obtain accurate line ratios, making no a priori assumptions about the beam-source coupling factor. For these reasons, in most of the objects observed with the NRAO 12 m telescope, we observed the ^{12}CO $J = 2$–1 emission in a rectangular nine-point grid with a cell

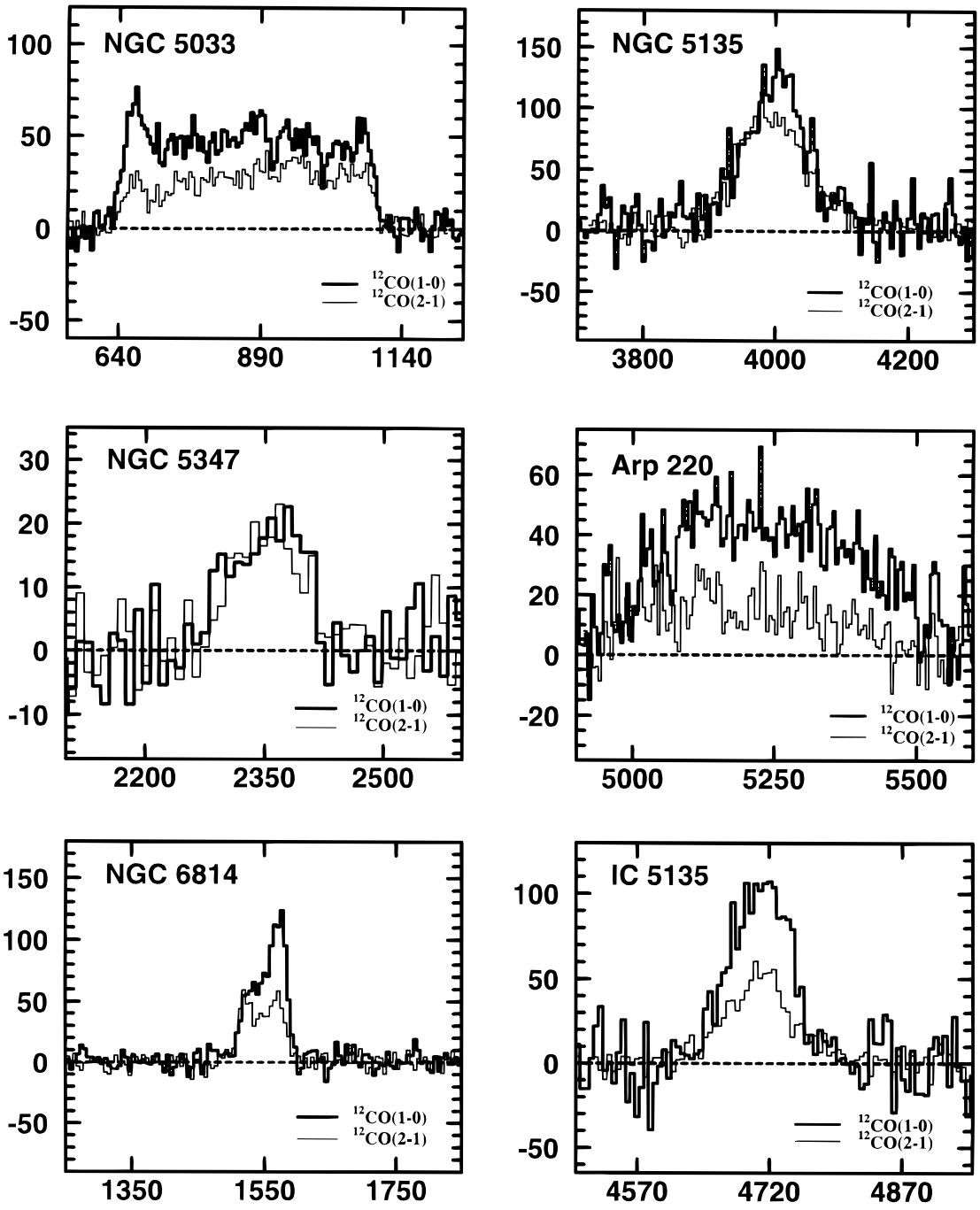

FIG. 1—*Continued*

size of 15″ and then convolved it to the resolution of our ^{12}CO $J = 1$–0 measurement. This procedure is described in detail in the Appendix.

We estimated the rms error associated with each line intensity measurement using the relation

$$\left(\frac{\delta T}{T}\right) = \left[\left(\frac{\delta T}{T}\right)^2_{\rm ther} + \left(\frac{\delta T}{T}\right)^2_{\rm drift} + \left(\frac{\delta T}{T}\right)^2_{\rm syst}\right]^{1/2}. \quad (1)$$

The first term in equation (1) expresses the thermal rms error. If T is the main-beam temperature averaged over $N_{\rm ch}$ channels, and if the baseline subtracted is defined more or less symmetrically around the line profile by a total number of $N_{\rm bas}$ channels, then

$$\left(\frac{\delta T}{T}\right)_{\rm ther} = \frac{\delta T_{\rm ch}}{T}\left(\frac{N_{\rm bas} + N_{\rm ch}}{N_{\rm bas} N_{\rm ch}}\right)^{1/2}, \quad (2)$$

where $\delta T_{\rm ch}$ is the thermal noise per channel, estimated for each individual spectrum.

The second term in equation (1) expresses the drift of the temperature scale due to all other errors of stochastic nature, e.g., variations of the physical temperatures of the calibrating loads or rapidly varying atmospheric opacity. In order to get an estimate of this source of error, we repeatedly observed many high signal-to-noise ratio (S/N) spectral

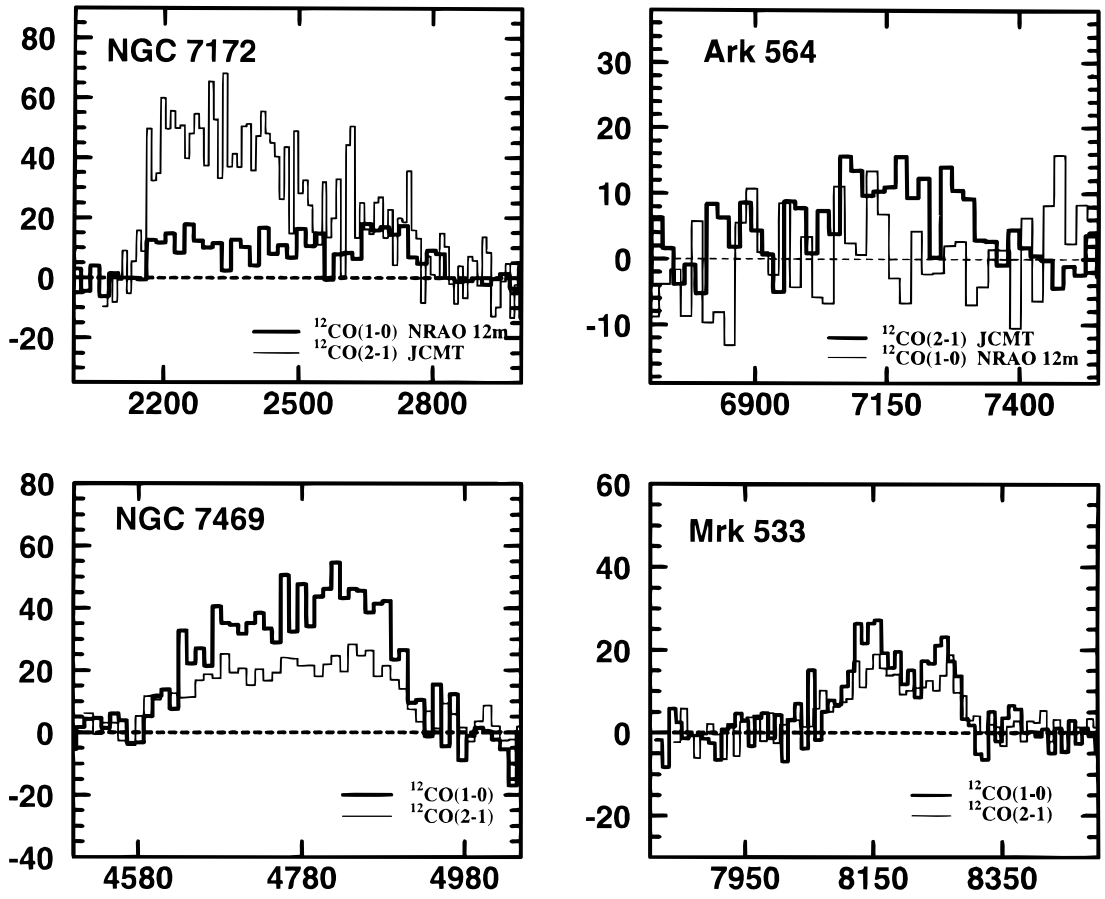

FIG. 1—*Continued*

lines of standard sources. The observed dispersion of their intensities is used to estimate the second term in equation (1) since, for these sources, the thermal rms error is negligible. In the case of the NRAO 12 m telescope, it was found to be ~ 0.10 at 115 GHz and ~ 0.15 at 230 GHz.

Finally, the third term in equation (1) expresses the systematic uncertainty introduced to the line intensities because of the (unavoidably) imprecise telescope efficiency factors used to deduce $T_{\rm mb}$. This term is systematic only in the sense that the same efficiency factors are used for all line intensities at a particular frequency and telescope, but it is uncorrelated to the other two terms in equation (1) and expresses the rms error associated with the measurement of the telescope efficiency factors. For the NRAO 12 m telescope, this term is of the order of ~ 0.10 for both frequencies (S. J. E. Radford 1996, private communication).

We note that in many cases in the literature only the thermal rms errors are reported (i.e., the first term of eq. [1]), which results in significant underestimates of the true error associated with millimeter spectral-line observations.

2.3. *JCMT Observations*

We also used the James Clerk Maxwell Telescope (JCMT)[2] in two observing runs between 1994 May 7 and 10, and between 1995 June 17 and 18 to observe the ^{12}CO, ^{13}CO $J = 2$–1 lines at 230 and 220 GHz, respectively, in some of the galaxies in our sample. The profile of the main beam of the telescope at these frequencies is closely approximated by a Gaussian beam with HPBW = 21″. Focus and pointing were monitored frequently by observing bright quasars and planets. The pointing error (rms) was found to be $\sim 4''$. The JCMT observations were performed by using beam switching at the recommended rate of 1 Hz and beam throws of 2′–3′ in azimuth. The DAS spectrometer was used with a total usable bandwidth of ~ 700 MHz corresponding to a velocity coverage of ~ 910 km s^{-1} at a spectral resolution of 0.625 MHz. We converted the measured temperature scale T_A^* of the JCMT spectra to the $T_{\rm mb}$ scale by using the relation $T_{\rm mb} = T_A^*/n_{\rm mb}$, adopting a beam efficiency of $n_{\rm mb} = 0.69$ (Matthews 1996) at 230 GHz. The baselines for the spectra were found to be both flat and stable during the observations.

The error is estimated according to equation (1), and observations of high S/N spectral-line standards show that the temperature scale drift factor is of the order of ~ 0.10 at 230 GHz. The systematic error is ~ 0.10 (G. Sandell 1995, private communication).

3. RESULTS

3.1. *The* ^{12}CO (2–1)/(1–0) *and* ^{12}CO/^{13}CO $J = 1$–0 *Line Ratios*

The line ratios estimated throughout this study are based on the main-beam brightness $T_{\rm mb}$ averaged over the entire FWZI of the line. This type of temperature scale is the one

[2] The James Clerk Maxwell Telescope is operated by the Observatories on behalf of the Science and Engineering Research Council of the United Kingdom, the Netherlands Organization for Scientific Research, and the National Research Council of Canada.

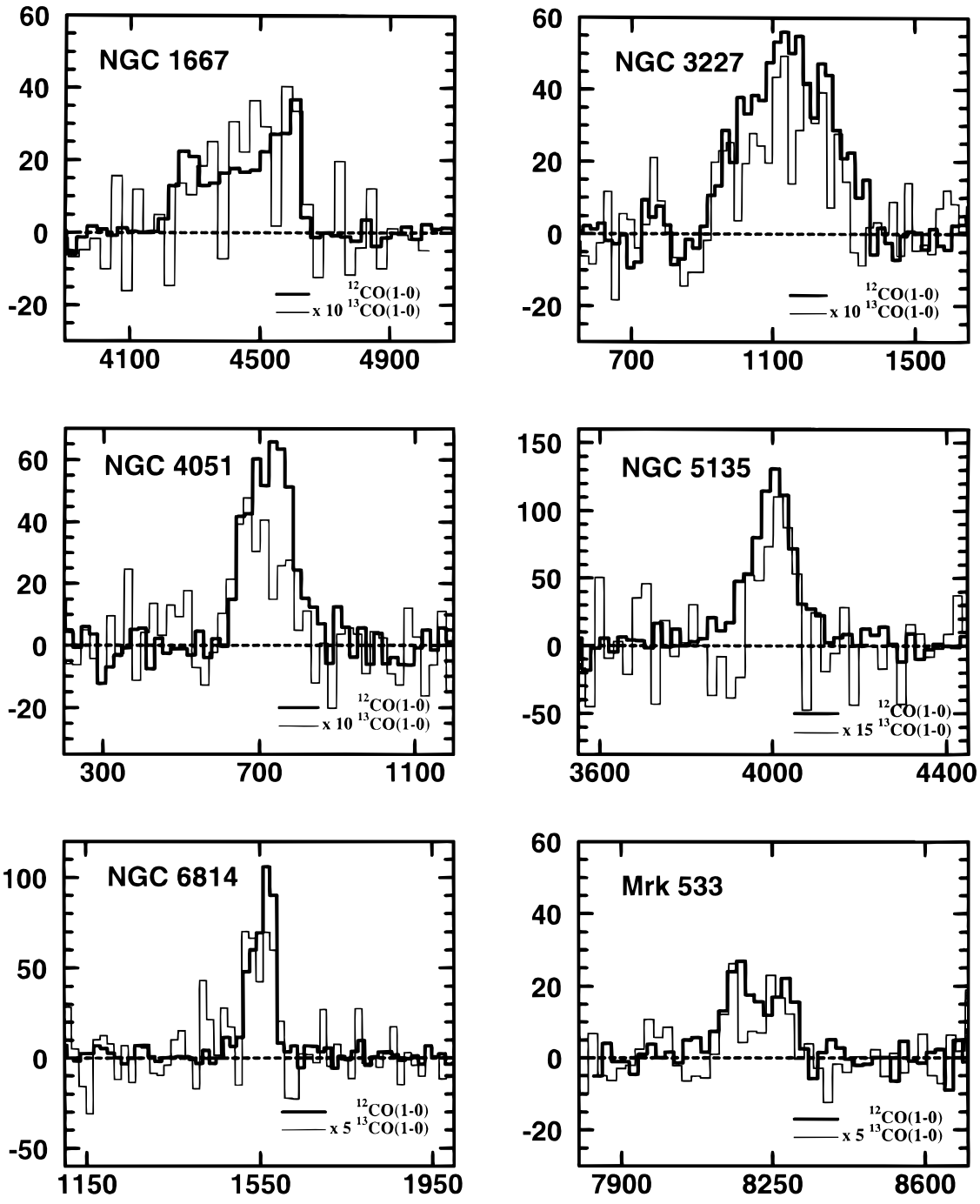

FIG. 2.—The ^{12}CO, ^{13}CO $J = 1$–0 spectra observed with the NRAO 12 m telescope. The velocity is in units of km s^{-1} (Heliocentric). The temperature is in units of millikelvin, and the temperature scale is T_{mb}.

appropriate for reporting our observations since all the galaxies are expected to have CO-emitting regions not much larger than the main beam of the telescopes that we used. This means that only the main beam will couple to the source and that T_{mb} is appropriately normalized by the main-beam solid angle Ω_{mb}. For most of the observed galaxies, the ^{12}CO $J = 2$–1 spectra were convolved to the resolution of the ^{12}CO $J = 1$–0 spectrum to estimate the $r_{12} = (2\text{–}1)/(1\text{–}0)$ ratio for ^{12}CO. The ^{12}CO, $J = 1$–0, $J = 2$–1 spectra of all the observed galaxies are displayed in Figure 1. The velocity scale for all the spectra is defined through the radio convention.[3]

Examining these spectra reveals that, in most cases, the two transitions exhibit similar line profiles, indicating that they both sample the same CO emission. In the only case (NGC 7172) where the velocity profiles did not agree, we

[3] In this convention, $V = c(v_0 - v)/v_0$, where v_0 and v are the rest and the observed frequencies, respectively.

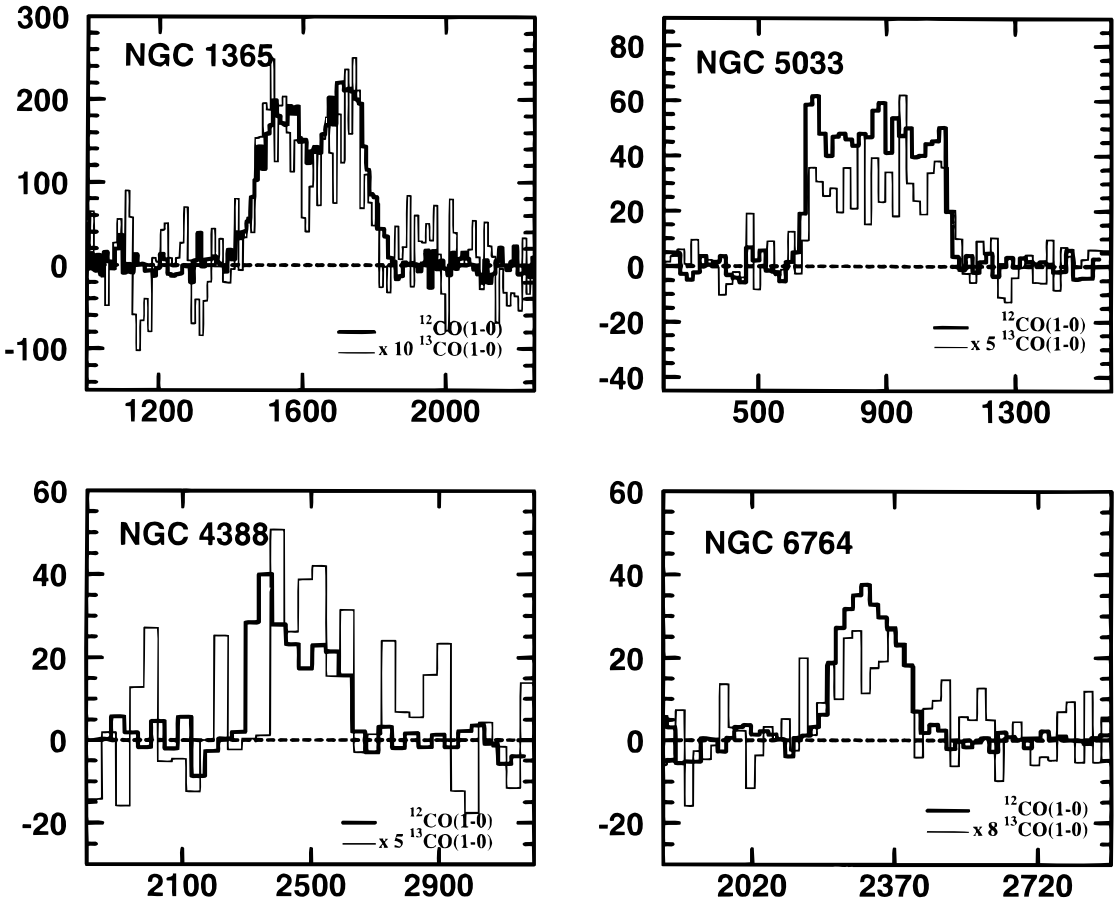

FIG. 2—*Continued*

did not estimate a line ratio. In this case, different beams were used, and the source's optical size indicates that the CO emission may be extended with respect to them.

In order to check for consistency with other observers, we compared our values of r_{12} with values found in the literature for Mrk 231 (Rigopoulou et. al 1996 and references therein), Arp 220 (Radford, Solomon, & Downes 1991; Aalto et al. 1995; Rigopoulou et al. 1996), the nearby LINER NGC 6764 (Eckart et al. 1991), NGC 3227, and NGC 5033 (Braine & Combes 1992). For the first four galaxies, we find excellent agreement within the reported errors, and only in the case of NGC 5033, we obtain very different values from Braine & Combes (1992), who find a ratio of $r_{12} \sim 1.6$, while we measure a much lower value of 0.58. However, the CO emission in NGC 5033 is extended on scales of $\sim 20''$–$60''$ (Meixner et al. 1990), and the velocity profile of our spectra in Figure 1 is very different than the one presented in Braine et al. (1993). This is a strong indication that the larger beam ($\sim 55''$) of the NRAO 12 m telescope samples different gas (more extended, colder?) than the beam ($\sim 23''$) of the 30 m IRAM telescope.

Note that in a few cases in the literature the spectra used to estimate r_{12} have been obtained with different resolutions. When the source size θ_s is less than that of the smallest beam used, the intrinsic line ratio $T_R(2\text{–}1)/T_R(1\text{–}0)$ can be determined reliably by using the equation:

$$r_{12} = \frac{T_R(2\text{–}1)}{T_R(1\text{–}0)} = n_c(\theta_s, \theta_{10}, \theta_{21}) \frac{T_{\rm mb}(2\text{–}1)}{T_{\rm mb}(1\text{–}0)}$$

$$= \left(\frac{\theta_s^2 + \theta_{21}^2}{\theta_s^2 + \theta_{10}^2}\right) \frac{T_{\rm mb}(2\text{–}1)}{T_{\rm mb}(1\text{–}0)}, \quad (3)$$

where n_c is the ratio of the beam-coupling factors. We assumed a Gaussian source with FWHM width θ_s and Gaussian HPBW main-beam widths θ_{10} and θ_{21} that correspond to the CO $J = 1$–0 and $J = 2$–1 transitions, respectively. Equation (3) shows that, unless the source is significantly smaller than the smaller beam used, the "deconvolved" line ratio depends heavily on the adopted source size. For example, assuming that $\theta_{10} \sim 2\theta_{21}$, the beam correction factor n_c can range from $n_c \sim \frac{1}{4}$ (point source) to $n_c \sim \frac{2}{5}$ ($\theta_s = \theta_{21}$). This is enough to change a "deconvolved" line ratio from $r_{12} \sim 0.90$ (for point source) to $r_{12} \sim 0.56$ (for $\theta_s = \theta_{21}$). Since the first value is usually found for warm ($T_{\rm kin} \gtrsim 20$ K), optically thick gas while the latter one is associated with cold and/or subthermally excited gas, it is obvious that deducing gas excitation properties in such cases would yield highly ambiguous results. For this reason, whenever we use line ratio data from the literature, we include only the ones that have been obtained with matched beams, with the use of fully sampled

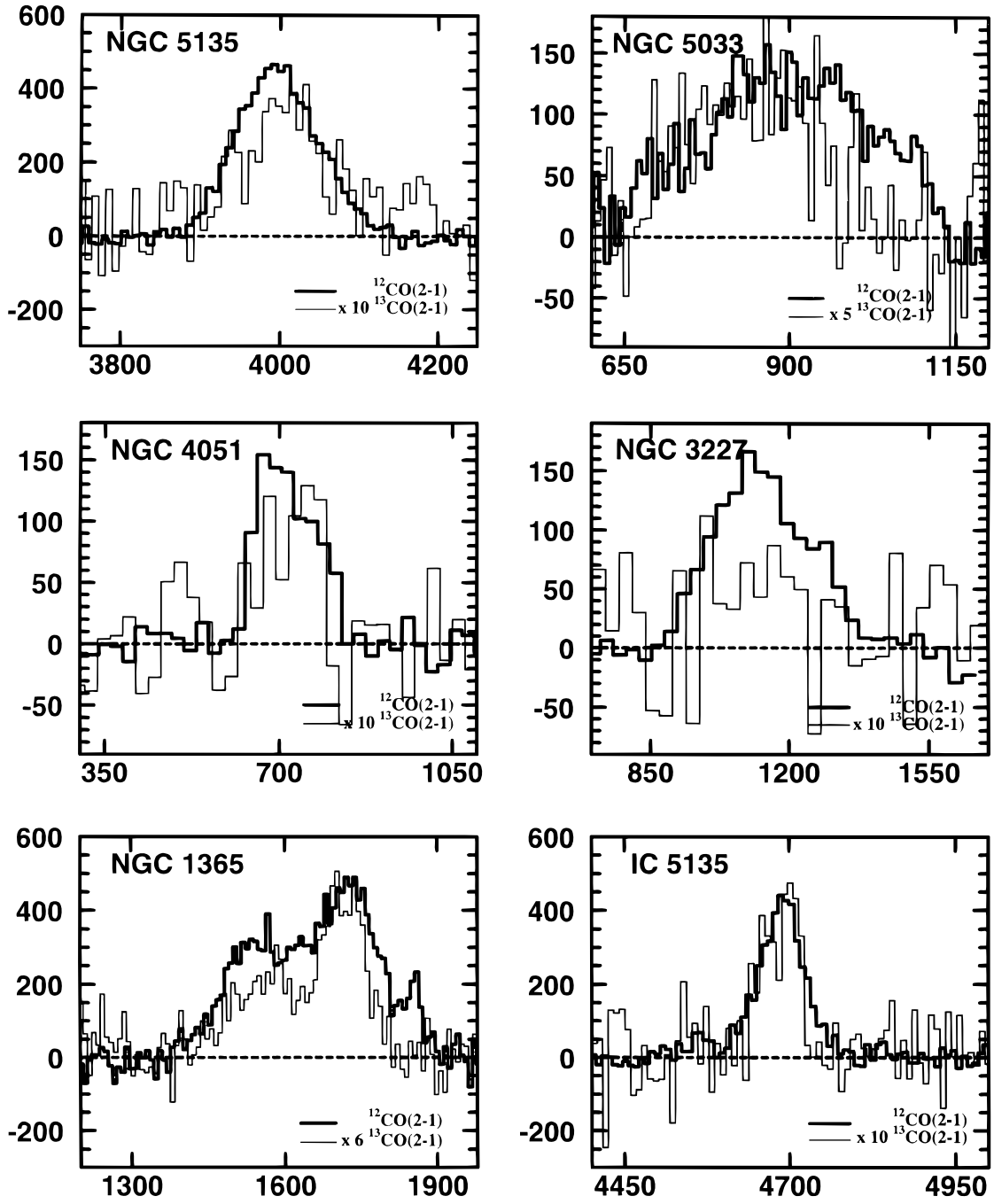

FIG. 3.—The ^{12}CO, ^{13}CO $J = 2$–1 spectra observed with the JCMT. The velocity is in units of km s^{-1} (Heliocentric). The temperature is in units of millikelvin, and the temperature scale is T_{mb}.

maps, or where the source is smaller than the smallest beam used.

The ^{12}CO, ^{13}CO $J = 1$–0 spectra obtained with the NRAO 12 m telescope are displayed in Figure 2. The ^{12}CO $J = 1$–0, $J = 2$–1, and ^{13}CO $J = 1$–0 measurements and the associated line ratios are presented in Table 1, together with the ratios found in the literature. In the few cases where more than one reliable measurement of r_{12} is available, we report the mean value and its associated formal error. In the case of Arp 220, the error reported is the dispersion of the observed values since, in most of its observations, the baseline is very poorly defined and the formal error is most likely an underestimate.

In the same table, we also display the quantity Ω_s/Ω_{mb}, where $\Omega_s = D_{25}(1) \times D_{25}(2)$ (D_{25} obtained from the Third Reference Catalogue [RC3; de Vaucouleurs et al. 1991]) is a measure of the optical size of the galaxy and $\Omega_{mb} = (\pi/4)\theta^2_{HPBW}$ is the main-beam solid angle of the telescope used for the particular observation.

Except for Arp 220, for all galaxies where the $R_{10} = {}^{12}\mathrm{CO}/{}^{13}\mathrm{CO}$ $J = 1$–0 line ratio is reported, the resolution is identical or very similar to the one used to measure the r_{12} ratio. In the case of Arp 220, the small size ($\lesssim 10''$; Scoville et al. 1991) of the CO emission with respect to the beams

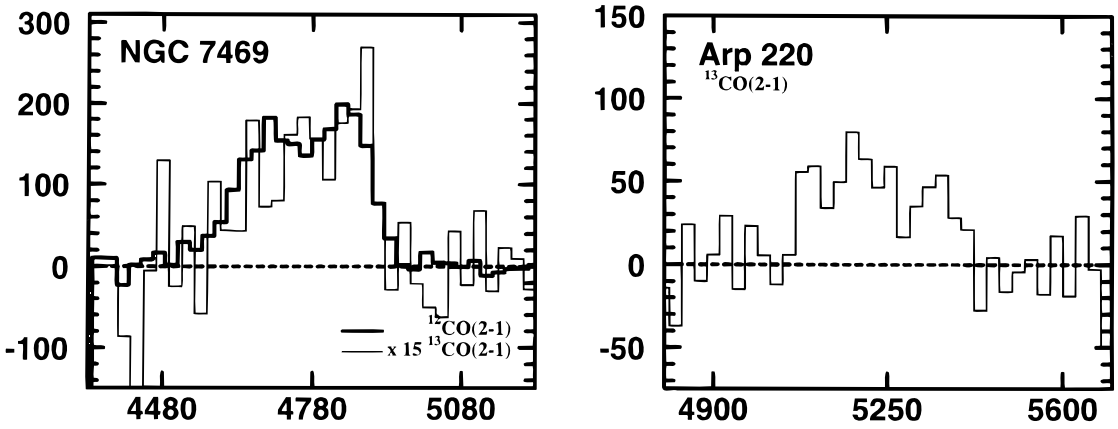

FIG. 3—*Continued*

used to obtain r_{12} (this work; Radford et al. 1991; Aalto et al. 1995; Rigopoulou et al. 1996) and R_{10} (Aalto et al. 1995) guarantees that these line ratios sample the same gas.

At the mean redshift $\langle z \rangle = 0.018$ of our Seyfert sample, the resolution of $\sim 55''$ corresponds to a projected linear size of $\langle L \rangle \sim 18$ kpc, and for most (21 out of 27) of the galaxies, it is $L \geq 6$ kpc. Hence, the line ratios r_{12} and R_{10} in this study usually probe the molecular gas properties averaged over a large area of each galaxy.

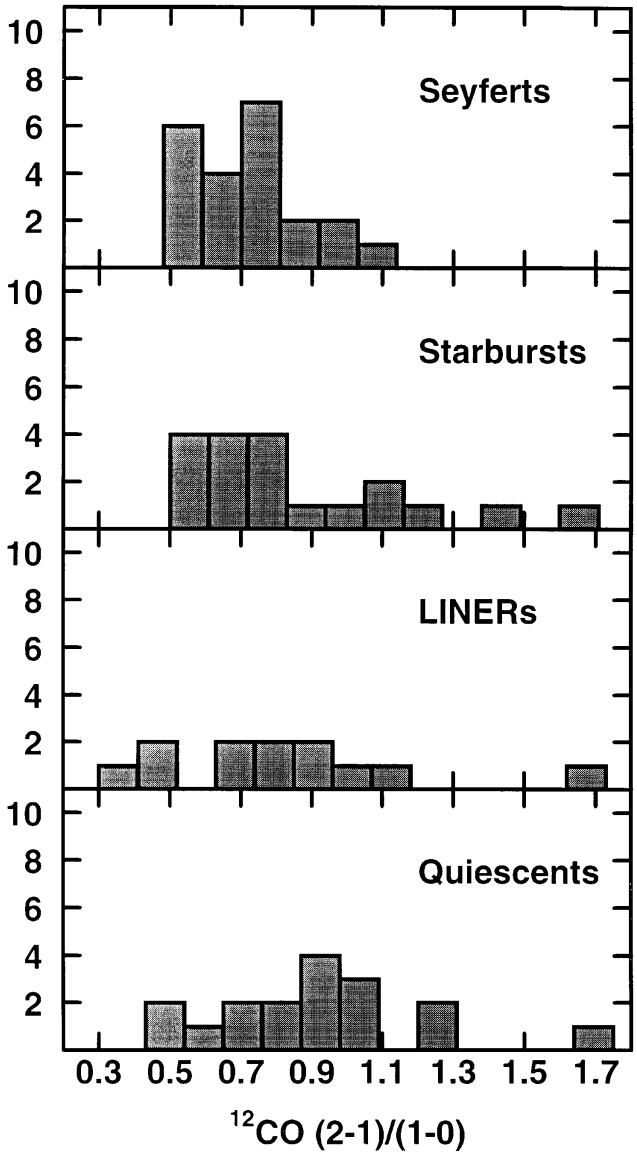

FIG. 4.—The frequency distribution of the $r_{12} = (2\text{–}1)/(1\text{–}0)$ ratio of ^{12}CO for Seyfert, starburst, LINER, and quiescent galaxies.

In order to extend our comparison of Seyfert galaxies to other classes of galaxies, we have searched the literature for extensive measurements of the r_{12} ratio. A summary of the relevant details of the various surveys used in the present study can be found in Table 2.

From the survey of CO line ratios in starburst galaxies by Aalto et al. (1995), we select only a small number of galaxies where similar values of the r_{12} have been obtained from two independent measurements with different telescopes. The reason for doing so is that, in their study, different beam sizes were used to obtain ratios by fitting Gaussians to the ^{12}CO $J = 2\text{–}1$ emission of extended sources and convolving to the resolution of the $J = 1\text{–}0$ transition. For the reasons mentioned previously, we do not consider this technique very reliable for sources whose size is comparable to the smallest of the two beams used, and even less so for a source that is extended with respect to that beam. In cases where a source has been observed more than once, we use the most reliable result, and if there is more than one reliable measurement, we report their mean value.

For the Seyfert galaxies in our sample, we find a mean (and the associated rms error of the mean) of $\langle r_{12} \rangle = 0.71 \pm 0.03$, while for each type separately, we find $\langle r_{12}(\text{Sy1}) \rangle = 0.69 \pm 0.04$ and $\langle r_{12}(\text{Sy2}) \rangle = 0.73 \pm 0.04$, implying no statistically significant difference between the two types. The average ^{12}CO/^{13}CO $J = 1\text{–}0$ line ratio for Seyfert galaxies is $\langle R_{10} \rangle = 12 \pm 1$, irrespective of Seyfert type. This value is identical to the average value found recently by Aalto et al. (1995) for the centers of most noninteracting starburst galaxies and similar to the ones found by Young & Sanders (1986) and Sage & Isbell (1991) for nearby spirals.

The galaxies NGC 5135, Arp 220, and to a lesser degree NGC 3227 seem to have values of the R_{10} ratio significantly higher than the mean, confirming earlier reports by Aalto et al. (1995) that high R_{10} ratios occur in strongly interacting or merging galaxies. Indeed, NGC 5135 belongs to a group of seven galaxies that are gravitationally bound and lie within 1 Mpc of one another, Arp 220 is thought to be an advanced merger (Sanders et al. 1988), and NGC 3227 is a well-known Seyfert galaxy interacting with NGC 3226 (Kukula et al. 1995).

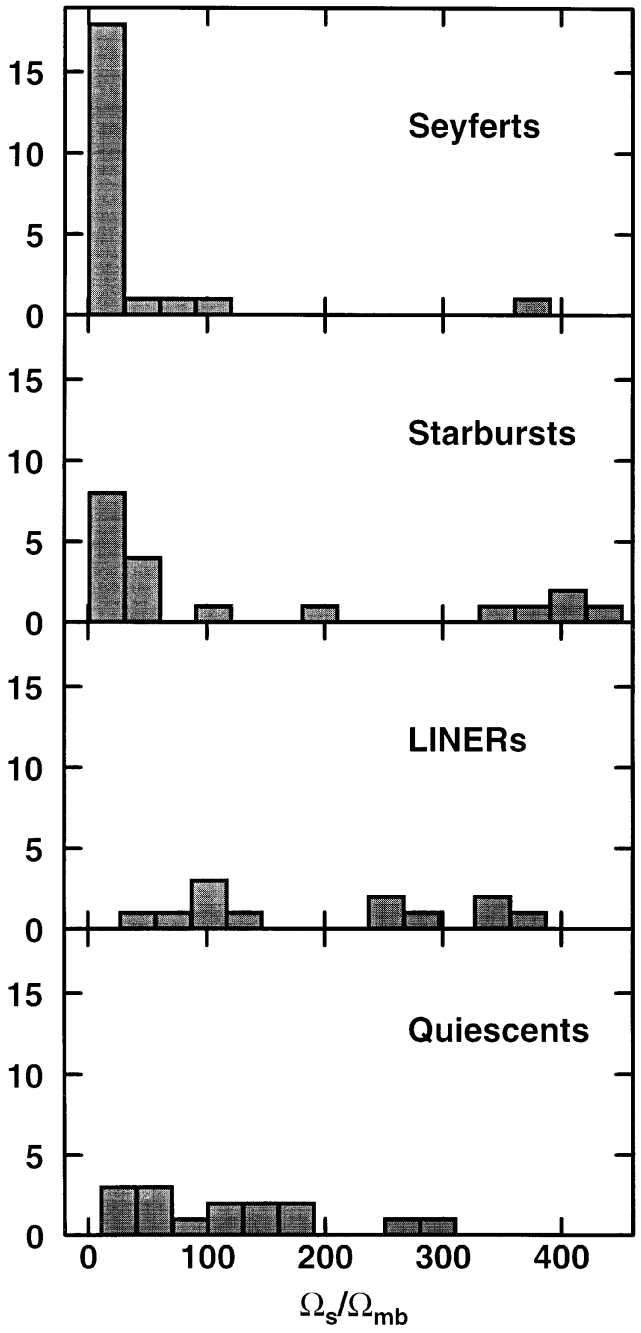

FIG. 5.—The frequency distribution of the Ω_s/Ω_{mb} ratio for Seyfert, starburst, LINER, and quiescent galaxies with measured r_{12} ratios. are The dimensions of the source at the surface brightness level of $\mu_B = 25.0B - mm/ss$ obtained from the RC3 are $\Omega_s = D_{25}(1) \times D_{25}(2)$, where $D_{25}(1, 2)$. The main beam of the telescope used is $\Omega_{mb} = (\pi/4)\theta^2_{HPBW}$.

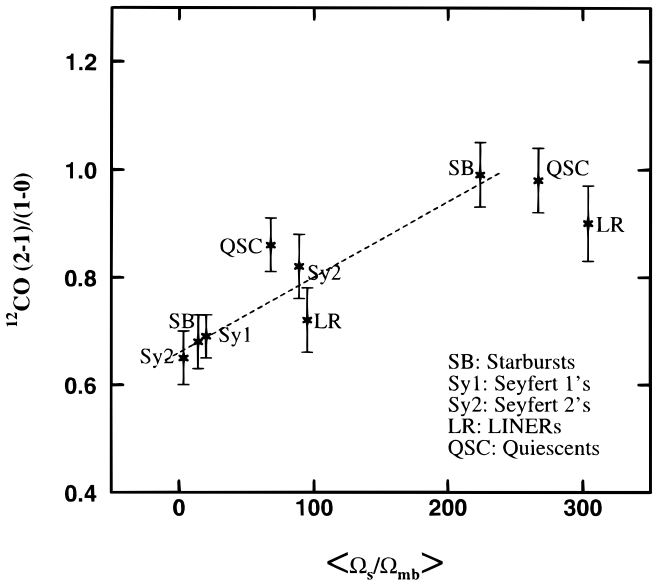

FIG. 6.—The average ^{12}CO $r_{12} = (2–1)/(1–0)$ line ratio vs. the average Ω_s/Ω_{mb} (see text). The error bars are a 1 σ standard deviation of the mean. The first seven points of the graph have a correlation coefficient of $r_{cor} = 90\%$, with a probability that their configuration arose by chance less than 5%. The line showing comes from eq. (6) (see text) for $L_s = 20$ kpc, $L_w = 0.9$ kpc. The line ratios are $r_{12}^{(w)} = 0.90$, $r_{12}^{(c)} = 0.66$, and $T_b(1–0)_{(w)}/T_b(1–0)_{(c)} = 3$. The following set of conditions can reproduce these ratios fairly closely. *Cold gas*: $T_{kin} = 9$ K, $n(H_2) = 10^3$ cm^{-3}, $X/(dV/dr) = 3 \times 10^{-5}$ (km s^{-1} pc^{-1})$^{-1}$ *Warm gas*: $T_{kin} = 26$ K, $n(H_2) = 3 \times 10^3$ cm^{-3}, $X/(dV/dr) = 3 \times 10^{-6}$ (km s^{-1} pc^{-1})$^{-1}$.

It has been suggested by Aalto et al. (1995) that R_{10} is a measure of molecular cloud disruption in starburst nuclei. According to this picture, the large molecular gas densities [$\Sigma(H_2) > 10^4\ M_\odot$ pc^{-2}] found in the centers of very IR-luminous ($L_{FIR} > 10^{11}\ L_\odot$) mergers lead to large pressures and turbulent line widths. This, together with the proximity of the circumnuclear gas to a steep gravitational potential, is responsible for generating a diffuse, optically thin [$\tau(^{12}CO) \approx 1$] molecular gas phase with $R_{10} \gtrsim 20$. In the same study, it has been proposed that intermediate ratios $10 \leq R_{10} \leq 15$ originate in the inner kiloparsec of less extreme starburst galaxies with more moderate gas surface densities [i.e., $\Sigma(H_2) \lesssim 10^3\ M_\odot$ pc^{-2}], and that small ratios $R_{10} \approx 6$ are a signature of a disk population of cold, optically thick molecular clouds residing in a quiescent environment.

It is interesting to note that, except for Arp 220, all the Seyfert galaxies in Table 1 with $R_{10} \lesssim 8$ also have $r_{12} \lesssim 0.7$. Following Aalto et al. (1995), we argue that these line ratios indicate that our large beam samples a significant part of the disk population of clouds in many of the galaxies in our sample. On the other hand, the archetypal Sy2 galaxy NGC 1068 with $r_{12} \sim 1$ (Braine & Combes 1992) has $R_{10} = 14$ for the inner $\sim 30''$, which is the approximate size of the central starburst (Wilson & Ulvestad 1982; Telesco et al. 1984; Telesco & Dreher 1988; Atherton, Reay, & Taylor 1985). The excitation of the molecular gas in this case may be more characteristic of gas residing in the circumnuclear regions of less extreme starburst galaxies.

We must also mention that high R_{10} ratios could be the result of an intrinsically high [^{12}CO/^{13}CO] abundance ratio (Casoli, Dupraz, & Combes 1992). Such abundances can be produced because of selective nucleosynthesis by massive stars (Henkel & Mauersberger 1993) and/or selective photodissociation of the ^{13}CO molecules in the UV-intense starburst environment (e.g., Fuente et al. 1993). These phenomena are expected to occur mainly in the inner regions of starburst galaxies rather than in the more quiescent disk, and their effect would be to introduce a wider range of values for R_{10} with respect to the r_{12} ratio that does not depend on the [^{12}CO/^{13}CO] abundance.

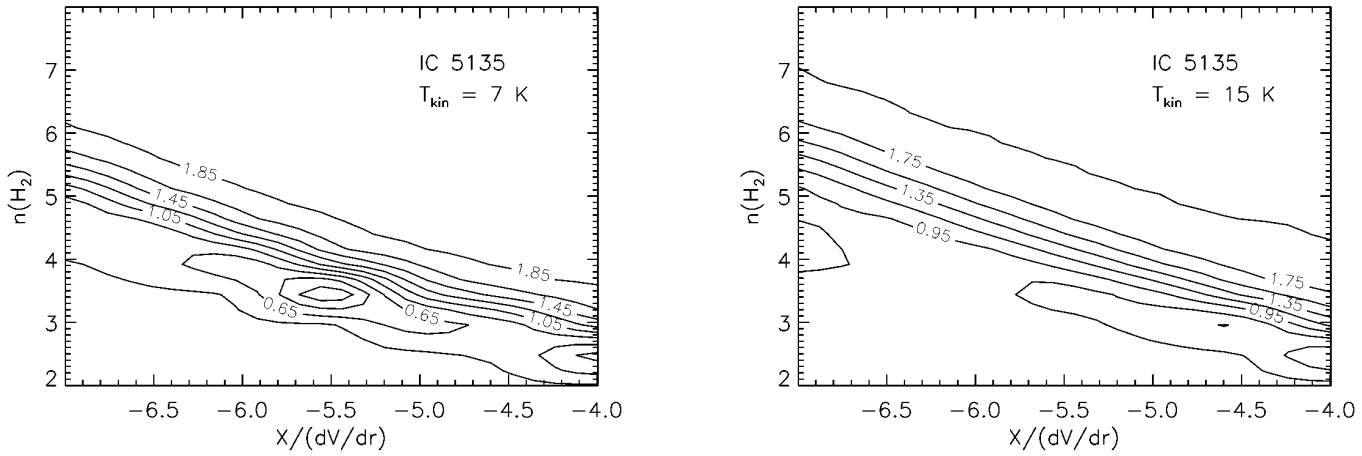

FIG. 7.—Two contour maps of log χ^2 with $T_{\rm kin} = 7$ and 15 K for IC 5135. The minimum value is log $\chi^2_{\rm min} = 0.056$ ($T_{\rm kin} = 7$ K), the contour spacing is $\Delta \log \chi^2 = 0.2$, and $n(H_2)$ and Λ are expressed in logarithmic scale in units of cm^{-3} and (km s^{-1} pc^{-1})$^{-1}$, respectively.

3.2. *The* ^{12}CO/^{13}CO $J = 2$–1 *Line Ratio*

The ^{12}CO, ^{13}CO $J = 2$–1 spectra obtained with the JCMT are shown in Figure 3. Table 3 presents the ^{12}CO, ^{13}CO $J = 2$–1 JCMT measurements and their ratios. We also list the quantity Q for all the galaxies (except I Zw 001), which is defined as follows:

$$Q = \frac{\int_{4\pi} P_n(\mathrm{JCMT}) T_R \, d\Omega}{\int_{4\pi} P_n(12\ \mathrm{m})_{\rm cn} \, T_R \, d\Omega} \Rightarrow Q = \left[\frac{\theta_{\rm mb}(\mathrm{JCMT})}{\theta_{\rm mb}(12\ \mathrm{m})}\right]^2 \times \frac{T_{\rm mb}(\mathrm{JCMT})}{T_{\rm cn}(12\ \mathrm{m})}, \quad (4)$$

where P_n(JCMT) and $\theta_{\rm mb}$(JCMT) are, respectively, the beam pattern and the corresponding HPBW for the JCMT telescope at a frequency of $\sim$215 GHz, while $P_n(12\ \mathrm{m})_{\rm cn}$ and $\theta_{\rm mb}(12\ \mathrm{m})$ are the effective beam pattern and the corresponding HPBW ($\sim 55''$) for the convolved spectrum (see Appendix) of the ^{12}CO (2–1) transition observed with the NRAO 12 m telescope. The quantities $T_{\rm mb}$ and T_R are the velocity-averaged main-beam brightness and intrinsic brightness temperatures of the ^{12}CO $J = 2$–1 transition, and $T_{\rm cn}(12\ \mathrm{m})$ is the convolved spectrum of ^{12}CO $J = 2$–1 obtained from the nine-point maps with the NRAO 12 m telescope. From the definition of Q, it is apparent that for sources resolved by the smaller JCMT beam $Q < 1$, while for the unresolved ones $Q \sim 1$.

Table 3 shows that IC 5135 and NGC 7469 are unresolved by the JCMT beam, and this is also the case for I Zw 001, the most distant Seyfert galaxy in our sample, since the telescope beams used (Barvainis, Alloin, & Antonucci 1989; Alloin et al. 1992; Eckart et al. 1994) were larger than the CO-emitting region. The statistics on the ^{12}CO/^{13}CO $J = 2$–1 ratio R_{21} is poorer than for R_{10} or r_{12}, but we find $\langle R_{21} \rangle = 13 \pm 1$, which is identical to the value found by Aalto et al. (1995) for their sample of starburst nuclei. The same mean value is found for Sy2 and Sy1 galaxies separately. Once again, we measure the highest values of R_{21} toward strongly interacting or merging galaxies like NGC 3227 and Arp 220.

For NGC 5135, the ratio $R_{21} = 13$ is significantly lower than $R_{10} = 26$ (Table 1). Even though for this galaxy Q is slightly less than unity, the profiles of the two spectra of the ^{12}CO $J = 2$–1 transition (Figs. 1 and 3) are very similar, so it is possible that the two beams sample the same gas. In such a case, the ^{13}CO (2–1)/(1–0) ratio is $r_{13} = (R_{10}/R_{21}) r_{12} = 1.7 \pm 0.5$, comparable, within the errors, to $\langle r_{13} \rangle = 1.3$ found by Aalto et al. (1995) toward the centers of starburst galaxies. The only other Seyfert galaxy unresolved by the JCMT beam with both $J = 2$–1, 1–0 transitions of ^{13}CO measured is IC 5135, a luminous ($L_{\rm FIR} \sim 10^{11}\ L_\odot$) far-infrared source. The nuclear region of this galaxy exhibits the characteristics of both a Sy2 and a very intense starburst galaxy (Shields & Fillipenko 1990). We find $r_{13} = 0.36 \pm 0.10$, a very low value when compared with the one measured for NGC 5135 and the mean value reported by Aalto et al. (1995). This value as well as $r_{12} = 0.50$ correspond to linear scales of $\sim$6 kpc ($\sim 21''$ at $z = 0.016$), and therefore it seems that, despite the intense nuclear activity in IC 5135, the global CO emission arises from cold ($T_{\rm kin} \lesssim 10$ K) and possibly subthermally excited

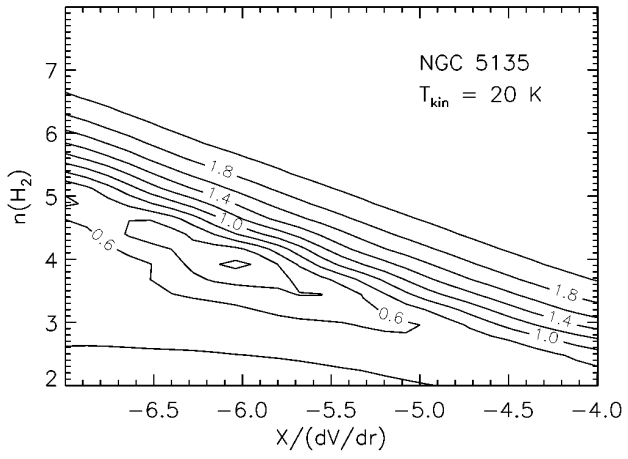

FIG. 8.—Contour map of log χ^2 with $T_{\rm kin} = 20$ K for NGC 5135. The minimum value is log $\chi^2_{\rm min} = 0.14$, the contour spacing is $\Delta \log \chi^2 = 0.2$, and $n(H_2)$ and Λ are expressed in logarithmic scale in units of cm^{-3} and (km s^{-1} pc^{-1})$^{-1}$, respectively.

TABLE 1

THE ^{12}CO $J = 2$–1, 1–0 AND ^{13}CO $J = 1$–0 DATA

Galaxy	Sy[a]	Ω_s/Ω_{mb}	^{12}CO (1–0)[b]	^{13}CO (1–0)[b]	^{12}CO (2–1)[c]	$\frac{^{12}\text{CO (1–0)}}{^{13}\text{CO (1–0)}}$ [d]	$\frac{^{12}\text{CO (2–1)}}{^{12}\text{CO (1–0)}}$ [d]
Mrk 938	2	3	10.1 ± 1.8	...	7.1 ± 1.6	...	0.80 ± 0.14[e]
NGC 1068	2	387	...	...	...	14 ± 2[f]	1.10 ± 0.20[g]
Mrk 348	2	6	6.2 ± 0.8	...	≤ 13.9	...	≤ 0.96[h]
NGC 1365	2	106	148.7 ± 20.8	11.7 ± 1.9	81.8 ± 8.1	13 ± 3	0.55 ± 0.09
NGC 1667	2	4	20.6 ± 3.1	2.1 ± 0.5	12.1 ± 1.7	10 ± 2	0.59 ± 0.10
MCG +8-11-11	1	14	4.3 ± 0.7	...	≤ 8.75	...	≤ 1.06[h]
NGC 2273	2	12	8.2 ± 1.2	...	7.4 ± 1.4	...	0.92 ± 0.15[e]
Mrk 10	1	2	2.3 ± 0.6	...	≤ 1.1	...	≤ 0.48
NGC 2992	2	6	13.4 ± 2.3	...	6.6 ± 0.8	...	0.49 ± 0.10
NGC 3227	1	30	32.6 ± 5.6	2.1 ± 0.4	27.6 ± 4.6	17 ± 3	0.77 ± 0.14[g]
NGC 4051	1	31	36.2 ± 5.1	2.8 ± 0.4	22.0 ± 3.0	13 ± 3	0.61 ± 0.11
NGC 4388	2	11	22.7 ± 3.4	4.0 ± 1.0	15.9 ± 1.7	6 ± 2	0.70 ± 0.13
Mrk 231	1	2	10.2 ± 1.7	...	9.6 ± 1.4	...	0.98 ± 0.10[i]
NGC 5033	1	82	46.2 ± 6.5	5.6 ± 0.7	27.1 ± 2.9	8 ± 1	0.58 ± 0.10
NGC 5135	2	7	66.9 ± 9.9	2.6 ± 0.4	57.1 ± 6.3	26 ± 5	0.85 ± 0.14
Mrk 273	2	10	...	...	...	...	0.80 ± 0.15[j]
NGC 5347	2	3	12.5 ± 2.2	...	11.0 ± 1.7	...	0.88 ± 0.21
Mrk 463	1	7	...	...	...	...	0.76 ± 0.15[k]
Arp 220	2	3	36.9 ± 5.1	...	13.3 ± 2.4	> 20[l]	0.53 ± 0.13[m]
NGC 6814	1	13	59.5 ± 8.2	8.1 ± 1.2	35.8 ± 3.9	7 ± 1	0.60 ± 0.10
IC 5135	2	3	61.7 ± 9.2	...	31.2 ± 3.7	8 ± 1[l]	0.50 ± 0.10
NGC 7469	1	3	35.0 ± 5.2	...	16.9 ± 2.2	...	0.48 ± 0.09
Mrk 533	2	2	13.7 ± 2.2	1.6 ± 0.4	10.6 ± 1.6	9 ± 2	0.77 ± 0.16
NGC 6764	LINER	5	24.9 ± 3.2	2.25 ± 0.49	24.5 ± 3.2	11 ± 3	0.98 ± 0.19
Ark 564	1	3	≤ 5.4	...	9.9 ± 2.4	...	≥ 0.50[h]
I Zw 001	1	7	...	...	...	9 ± 2[n]	0.73 ± 0.11[o]
Mrk 817	1	10	...	...	...	...	0.72 ± 0.14[k]

[a] Seyfert type.
[b] The velocity-averaged main beam brightness $\langle T_{mb}(v)\rangle_{FWZI}$ (mK).
[c] The velocity-averaged convolved spectrum $\langle T_{cn}(v)\rangle_{FWZI}$ (mK).
[d] The ratio of the respective $\langle T_{mb}(v)\rangle_{FWZI}$'s.
[e] The mean of two values of ^{12}CO (2–1) observed with the NRAO 12 m telescope and JCMT.
[f] Papadopoulos, Seaquist, & Scoville 1996.
[g] NGC 1068: Braine & Combes 1992; NGC 3227: this work and Braine & Combes 1992.
[h] One ^{12}CO (2–1) measurement was taken; the assumed source size is $\theta_s \leq \frac{1}{3}\langle\theta_{opt}\rangle$.
[i] This work and values quoted in Rigopoulou et al. 1996.
[j] Rigopoulou et al. 1996.
[k] Alloin et al. 1992.
[l] Aalto et al. 1995.
[m] This work, Radford et al. 1991, Aalto et al. 1995, and Rigopoulou et al. 1996.
[n] Eckart et al. 1994.
[o] Barvainis et al. 1989 and Alloin et al. 1992.

gas (see § 4.2). In the next section, we discuss the possibility that such low line ratios in IR-luminous galaxies are solely due to a large filling factor of an extended cold gas phase with respect to a warm gas phase that is confined in the inner 0.5–1 kpc.

4. DISCUSSION

The low mean ratio $\langle r_{12}\rangle = 0.71$ found for Seyfert galaxies with respect to $\langle r_{12}\rangle = 0.90$ found toward the centers of nearby spiral (Braine & Combes 1992) and starburst gal-

TABLE 2

OBSERVATIONS OF ^{12}CO (2–1)/(1–0)

Reference	N_1[a]	Technique[b]	N_2[c]	Type of Galaxy[d]
This work	27	Nine-point grid, $\theta_s < \theta_{min}$	22	Seyfert
Braine & Combes 1992	36	Nine-point grid	34	Various
Chini, Krugel, & Steppe 1992	9	Matched beams	4	Starburst
Aalto et al. 1995	22	Multiple observations	3	Starburst
Radford et al. 1991	4	$\theta_s < \theta_{min}$	2	Starburst/AGN
Casoli et al. 1988	2	$\theta_s < \theta_{min}$	1	Starburst
Various studies[e]	10	Matched beams, maps[f]	4	Starburst

[a] The number of galaxies in the original sample.
[b] The observing technique used for the galaxies we select.
[c] The number of galaxies selected.
[d] Type of activity of the galaxies selected: various = starburst, LINER, quiescent galaxies.
[e] For a summary see Aalto et al. 1995 (p. 375 and references therein).
[f] Maps = a fully sampled ^{12}CO (2–1) map convolved to the resolution of a ^{12}CO (1–0) map.

TABLE 3

THE ^{12}CO, ^{13}CO $J = 2$–1 DATA

Galaxy	Sy[a]	^{12}CO (2–1)[b]	^{13}CO (2–1)[b]	$\frac{^{12}\text{CO (2–1)}}{^{13}\text{CO (2–1)}}$ [c]	Q
NGC 1365.....	2	314.5 ± 37.7	32.5 ± 4.2	10 ± 2	0.55 ± 0.10
NGC 3227.....	1	127.5 ± 15.3	5.01 ± 1.4	25 ± 8	0.68 ± 0.15
NGC 4051.....	1	130.1 ± 16.9	9.13 ± 2.2	14 ± 4	0.55 ± 0.11
NGC 5033.....	1	104.1 ± 12.5	16.3 ± 3.5	6 ± 1	0.54 ± 0.09
NGC 5135.....	2	320.3 ± 41.6	25.2 ± 3.5	13 ± 2	0.81 ± 0.14
Arp 220.....	2	...	3.2 ± 0.6	18 ± 3[d]	...
IC 5135.....	2	356.6 ± 42.8	33.3 ± 4.3	11 ± 2	1.10 ± 0.20
NGC 7469.....	1	137.2 ± 17.8	9.3 ± 2.3	15 ± 4	1.04 ± 0.21
I Zw 001.....	1	...	...	≥6[e]	...

[a] Seyfert type.
[b] The velocity-averaged main beam brightness $\langle T_{mb}(v)\rangle_{FWZI}$, in units of millikelvin.
[c] The ratio of the respective $\langle T_{mb}(v)\rangle_{FWZI}$'s.
[d] The mean of two values estimated from a NRAO 12 m telescope and IRAM ^{12}CO (2–1) measurement (Radford et al. 1991) and a JCMT ^{13}CO (2–1) measurement. The assumed source size is $\theta_s = 10''$.
[e] Eckart et al. 1994.

TABLE 4

K-S TEST RESULTS

Sample Pair	$(\Omega_s/\Omega_{mb})_{max}$ [a]	N_e [b]	D_m [c]	$Q_{KS}(D_m, N_e)$ [d] (%)
Seyfert and starburst galaxies	Whole range	10	0.27	35
	100	7	0.25	89
	50	6	0.17	99
Seyfert and quiescent galaxies.....	Whole range	10	0.45	3
	200	9	0.49	3
	100	5	0.66	1

[a] The maximum value of Ω_s/Ω_{mb} of the samples compared.
[b] $N_e = N_1N_2/(N_1 + N_2)$ is the effective number of data points. The K-S test is applicable for $N_e \geq 4$ (Stephens 1970).
[c] $D_m = \max S_1(x) - S_2(x)$ and $S_1(x)$, $S_2(x)$ are the two cumulative distribution functions.
[d] The K-S significance estimator.

axies (Aalto et al. 1995 and references therein) may signify a difference in their respective molecular gas excitation. Indeed, for many Seyfert galaxies observed (10 out of 26), we measure values of r_{12} as low as ~0.5–0.6. Assuming optically thick and thermalized levels up to $J = 2$, a ratio $r_{12} = 0.7$ corresponds to an excitation temperature of $T_{ex} = 7$ K that can probably be maintained by cosmic-ray heating (Goldsmith & Langer 1978). Hence, the ratios r_{12} observed for Seyfert galaxies correspond to either very cold and thermalized gas or (when $r_{12} < 0.7$) subthermally excited gas. This is in contrast with the warm ($T_{kin} \gtrsim 20$ K), optically thick gas that is usually associated with $r_{12} \sim 0.90$.

TABLE 5

IC 5135: LVG MODEL RESULTS

r_{12} [a] ($r_{12}^{(LVG)}$)	R_{10} [a] ($R_{10}^{(LVG)}$)	R_{21} [a] ($R_{21}^{(LVG)}$)	T_{kin} (K)	χ^2_{min} [b] [T_{kin}, $n(H_2)$, Λ]
0.50	8	11	5→16	1.14
(0.60).....	(8)	(15)		(7, 3, 3)
0.50	8	11	17→26	2.54
(0.63).....	(10)	(21)		(17, 0.3, 100)
0.60	9	9	7→16	1.46
(0.67).....	(9)	(16)		(9, 3, 3)
0.60	9	9	17→26	2.05
(0.84).....	(9)	(15)		Wide range[c]

NOTE.—For the grid of the LVG models, we used the increments $\Delta T_{kin} = 1$ K, $\Delta \log n(H_2) = 0.5$, and $\Delta \log \Lambda = 0.5$. The density range is $n(H_2) = (0.1 \rightarrow 10^5) \times 10^3$ cm^{-3}, and $\Lambda = X/(dV/dr) = (0.1 \rightarrow 10^2) \times 10^{-6}$ (km s^{-1} pc^{-1})$^{-1}$. The fit was performed by minimizing $\chi^2 = \sum_i (1/\sigma_i)[R^{(i)}_{obs} - R^{(i)}_{theor}]^2$, where $R^{(i)}_{obs}$ and σ_i are the observed line ratios and their associated 1 σ errors, respectively, and $R^{(i)}_{theor}$ are the theoretical ones deduced from the LVG model.

[a] The estimated line ratios from the LVG model with the smallest χ^2.
[b] The minimum value of χ^2 and the corresponding LVG parameters in units of kelvins, 10^3 cm^{-3}, and 10^{-6} (km s^{-1} pc^{-1})$^{-1}$.
[c] The χ^2_{min} found for every T_{kin} is almost constant.

Intuitively, one expects the gas in actively star-forming galaxies to be warmer than in quiescent ones since the intense UV radiation from massive stars and the enhanced gas turbulence present especially in starburst nuclei are expected to heat the gas. From this perspective, the lower values of r_{12} observed in Seyfert galaxies seem to contradict the notion that Seyfert galaxies as a whole have elevated rates of star formation compared with similar field galaxies (Maiolino et al. 1995). However, a problem with such a straightforward interpretation arises from the fact that the beams used in the various measurements of the r_{12} line ratio correspond to different linear sizes in different galaxy samples. In the case where a radial gas excitation gradient is present across a galaxy, different r_{12} ratios will then be measured for different beam sizes.

Figures 4 and 5 show the frequency distributions of r_{12} and Ω_s/Ω_{mb}, respectively, for four classes of galaxies, namely, Seyfert, starburst, LINER, and quiescent (i.e., with no AGN or prominent starburst).

TABLE 6

NGC 5135, AVERAGE STARBURST: LVG MODEL RESULTS

Galaxy	r_{12}, r_{13}, R_{10} [a] ($r_{12}^{(LVG)}$, $r_{13}^{(LVG)}$, $R_{10}^{(LVG)}$)	[T_{kin}, $n(H_2)$, Λ] [b]	τ_{10} [c]	T_{ex}/T_{kin} [d]	χ^2_{min}
NGC 5135	0.85, 1.70, 26 (0.99, 1.60, 23)	[20, 10, 1]	1.7	1.46	1.4
Average starburst.....	0.90, 1.30, 10 (0.90, 1.11, 10)	[27, 3, 10]	3.6	1.36	0.53
	0.90, 1.30, 15 (0.86, 1.16, 15)	[14, 10, 1]	3.1	1.20	0.44

NOTE.—The grid of LVG models used is the same as in Table 5, except for the temperature range where $T_{kin} = 8 \rightarrow 65$ K with $\Delta T_{kin} = 2$ K.

[a] The observed line ratios and the line ratios estimated from the LVG model with the smallest χ^2.

[b] The [T_{kin}, $n(H_2)$, Λ]-parameters (with the same units as in Table 5) that give the best fit.

[c] The optical depth of the ^{12}CO $J = 1$–0 transition.

[d] T_{ex} is the excitation temperature of the ^{13}CO, $J = 1$–0 transition.

From Figure 4, it is apparent that Seyfert galaxies have systematically lower line ratios than quiescent galaxies, and a similar trend is seen for the sample of starburst galaxies, although in their case, r_{12} does span the whole range of values found for the sample of quiescent galaxies. The LINERs and, even more so, the quiescent galaxies seem to be more uniformly distributed around the value $\langle r_{12} \rangle \approx 0.9$. A comparison of the frequency distributions of r_{12} and Ω_s/Ω_{mb} in Figures 4 and 5 reveal a broad correlation between these two variables in the case of Seyfert and starburst galaxies, where there seems to be a strong tendency for r_{12} and Ω_s/Ω_{mb} to cluster toward the lower end of their distributions. From the same figures, we see that similar trends, if they exist, are much less pronounced in the samples of LINERs and quiescent galaxies.

A gas excitation gradient consisting of warm gas in the central regions and cold gas in the outer regions can easily account for these effects. In such a case, a small beam will sample predominantly the warm nuclear component producing high r_{12} ratios while a larger beam will average in cold gas, thus resulting in lower observed r_{12} ratios.

Such molecular gas excitation gradients in galaxies have already been found in numerous cases. In particular, studies of the molecular gas in the center of the Galaxy (Gusten et al. 1985; Bally et al. 1988; Stark et al. 1991; Binney et al. 1991; Spergel & Blitz 1992) have revealed that the environment there is more extreme in terms of kinematics and gas excitation compared with the more quiescent disk. A similar picture emerges for the center and the disk of other galaxies (e.g., Knapp et al. 1980; Wall & Jaffe 1990; Wall et al. 1991, 1993; Eckart et al. 1991; Harris et al. 1991; Wild et al. 1992; Aalto et al. 1995), particularly for starbursts where intense star formation activity is found within the inner kiloparsec (e.g., Scoville et al. 1991; Wynn-Williams & Becklin 1993), and it is likely to heat the molecular gas.

The effect of such gradients to the observed r_{12} ratios is even better demonstrated in Figure 6 where the averages $\langle r_{12} \rangle$, $\langle \Omega_s/\Omega_{mb} \rangle$ for whole classes of galaxies are plotted. To a certain extent, such averaging is expected to "smooth out" the particular details of the gas excitation gradient that can be different in individual galaxies while retaining only its broader features that are expected to be common.

Assuming that the cold gas phase fills up the telescope beam and that the filling factor of the warm gas in the inner region is $f_w = \Omega_w/\Omega_{mb}$, then the observed r_{12} line ratio can be expressed as follows:

$$r_{12} = r_{12}^{(c)} \left\{ \frac{1 + f_w [T_b(2\text{–}1)_{(w)}/T_b(2\text{–}1)_{(c)}]}{1 + f_w [T_b(1\text{–}0)_{(w)}/T_b(1\text{–}0)_{(c)}]} \right\}, \quad (5)$$

where (c) = cold gas phase, (w) = warm gas phase, and T_b is the brightness temperature.

It is $f_w = (L_w/L_{mb})^2$, where L_w is the diameter of the central star-forming region, and L_{mb} the projected linear diameter corresponding to the telescope main beam. In most cases, we expect $f_w \ll 1$; hence, for reasonable temperature ratios between the warm and the cold gas phase, we can approximate equation (5) and write it as follows:

$$r_{12} = \left[(r_{12}^{(w)} - r_{12}^{(c)}) \left(\frac{L_w}{L_s} \right)^2 \frac{T_b(1\text{–}0)_{(w)}}{T_b(1\text{–}0)_{(c)}} \right] x + r_{12}^{(c)}, \quad (6)$$

where we have set $f_w = (L_w/L_s)^2 x$, with $x = (L_s/L_{mb})^2 = \Omega_s/\Omega_{mb}$.

In Figure 6, it is shown that, for a typical set of parameters characterizing the warm and the cold gas phase, equation (6) easily accounts for the correlation between $\langle r_{12} \rangle$ and $\langle \Omega_s/\Omega_{mb} \rangle$. Predictably, the fit seems to fail when the projected linear size of the beam becomes $L_{mb} \sim 1$ kpc ($x \sim 250$), i.e., comparable to the typical size of a nuclear starburst.

4.1. *A Similar Gas Excitation Gradient for Seyfert and Starburst Galaxies?*

The previous discussion makes it apparent that caution is needed when using observed line ratios to demonstrate differences or similarities in molecular gas properties among galaxies over large scales. Nevertheless, there are some indications that Seyfert galaxies may be sharing more common features in their global gas excitation conditions with starburst rather than quiescent galaxies. The frequency distributions of r_{12} (Fig. 4) for Seyfert and starburst galaxies seem to be similar in their overlapping region. The results from a Kolmogorov-Smirnov (K-S) test performed for the distribution of r_{12} in Seyfert, starburst, and quiescent galaxies are shown in Table 4.

In this table, we see that the probability Q_{KS} that the two samples of r_{12} for Seyfert and starburst galaxies are drawn from the same distribution increases up to 99% as we restrict the range of Ω_s/Ω_{mb} of the samples to lower values where most of the Seyfert galaxies are found. On the con-

trary, a similar comparison between Seyfert and quiescent galaxies yields $Q_{KS} \lesssim 3\%$.

This picture is consistent with the notion that Seyfert and starburst galaxies are more likely to harbor an intense nuclear ($\lesssim 1$ kpc) starburst that warms the gas in that region while more quiescent types harbor star formation that is usually more spread out in the disk, thus establishing a somewhat different pattern of global molecular gas excitation.

4.2. *Molecular Gas in Seyfert Galaxies: Cold Gas Phase*

In order to probe the properties of the cold gas component, we chose IC 5135 (Sy2) as our template galaxy. The reason is twofold: (1) the low line ratio r_{12} implies that its CO emission is dominated by very cold and/or subthermally excited gas, and (2) the transitions ^{12}CO $J = 1$–0, $J = 2$–1 observed with the NRAO 12 m telescope and the transitions ^{13}CO, ^{12}CO $J = 2$–1 observed with the JCMT seem to sample the same gas ($Q \sim 1$) over scales of ~ 6 kpc. Hence, they can be used together to constrain the average gas properties over a large area of this galaxy.

The line ratios $r_{12} = 0.50 \pm 0.10$ and $R_{10} = 8 \pm 1$ observed in IC 5135 are considered characteristic of a disk population of clouds (e.g., Aalto 1994; Aalto et al. 1995; Eckart et al. 1991). The $R_{21} = 11 \pm 2$ measured with the JCMT corresponds to $r_{13} = (R_{10}/R_{21}) r_{12} = 0.36 \pm 0.11$. Line ratios as low as these are a strong indication of subthermal excitation since the assumption of thermal excitation (LTE) of the levels up to $J = 2$ leads to $T_{kin} = 4$ K, which is below the minimum value of $T_{min} \sim 7$ K that can be sustained by cosmic-ray heating (Goldsmith & Langer 1978). Allen & Lequeux (1993) have reported observations of the ^{12}CO $J = 1$–0, 2–1 transitions from two dust clouds in the inner disk of M31 where they find massive (few times $10^7\ M_\odot$) molecular clouds with $r_{12} = 0.3$–0.4, similar to the r_{12} and r_{13} ratios that we measure for the *global* ($\gtrsim 6$ kpc) CO emission in IC 5135. Allen et al. (1995) conclude that the properties of such clouds can be understood as resulting mainly from a very low UV radiation field and cosmic-ray density that allow the average kinetic temperature to drop to very low ($T_{kin} \lesssim 5$ K) values. For such conditions, an LTE solution that fits the observed line ratios in IC 5135 is still viable, but unlike non-LTE solutions, it is not density sensitive since it can correspond to any $n(H_2) \gtrsim 10^4$ cm^{-3}, the thermalization density of the $J = 2$–1 transition in the optically thin regime.

An adequate description of subthermal excitation conditions requires a full solution of the rate equations for the populations of the rotational energy levels of CO. For this purpose, we used a large velocity gradient (LVG) model by Richardson (1985), where it is assumed that the systematic motions rather than the local thermal velocities dominate the observed line widths of the molecular clouds. This greatly simplifies the solution of the rate equations since photons can interact with the radiating gas only locally. The model employed here assumes spherical clouds that collapse according to the velocity law $V(r) \propto r$, and it includes the rate equations for three CO isotopes and rotational levels up to $J = 10$. It has been shown (e.g., de Jong, Chu, & Dalgarno 1975; Richardson 1985) that different cloud geometries (plane vs. spherical) and velocity laws result in variations of the deduced molecular gas properties that are less than or of the order of the typical observational errors. Throughout our modeling, we assume an abundance of $[^{12}CO/^{13}CO] = 60$ (Langer & Penzias 1993).

For the case of IC 5135, we have conducted a wide search of the LVG parameter space [T_{kin}, $n(H_2)$, Λ], where $\Lambda = X(dV/dr)^{-1}$, with $X = [^{12}CO/H_2]$ being the abundance of ^{12}CO relative to H_2, and dV/dr being the velocity gradient. Then we employed a χ^2 minimization technique in order to find the optimum set of parameters that reproduces the measured r_{12}, R_{10}, and R_{21} line ratios. The results are summarized in Table 5.

We find that the best fit corresponds to cold gas ($T_{kin} = 7$ K) with optically thick ($\tau_{10} \sim \tau_{21} \sim 10$) and thermalized ^{12}CO emission. The significant optical depth of this isotope and the resulting radiative trapping thermalizes its emission up to the $J = 2$ level at an effective critical density $n(H_2)^*_{crit} \sim n(H_2)_{crit}(J = 2\text{–}1)/\tau_{21} \sim 10^3$ cm^{-3}. For the same set of conditions, the ^{13}CO isotope is found to be optically thin ($\tau_{10} \sim \tau_{21} \sim 0.2$), with its $J = 2$–1 transition subthermally excited [$T_{ex}(2\text{–}1)/T_{kin} = 0.60$] as expected. Table 5 also shows that, even if we adopt the "warmest" values $r_{12} = 0.6$, $R_{10} = R_{21} = 9$ (so that $r_{13} = 0.6$) allowed by the errors, the optimum set of parameters [T_{kin}, $n(H_2)$, Λ] do not change except for the gas temperature, which nevertheless remains low.

The contour maps in Figure 7 display the contours of log χ^2 overlaid on the parameter space [$n(H_2)$, Λ] for $T_{kin} = 7$ and 15 K.

Cold and very likely subthermally excited gas also seems to dominate the emission in the Sy1 galaxy NGC 7469 where we measure $r_{12} = 0.48$ (Table 1). This galaxy, like IC 5135, is unresolved ($Q \sim 1$) by the JCMT beam, and thus the r_{12} (NRAO 12 m) and R_{21} (JCMT) ratios probe the same beam-averaged physical properties of the gas. An LTE solution corresponds to $T_{kin} = 3$–4 K, while a typical non-LTE solution from our LVG modeling is $T_{kin} = 10$ K and $n(H_2) \sim 3 \times 10^2$ cm^{-3}, $\Lambda \sim 1 \times 10^{-4}$ (km s^{-1} pc^{-1})$^{-1}$.

4.3. *Molecular Gas in Seyfert Galaxies: Warm Gas Phase*

Unlike the cold molecular gas residing in the more quiescent disk environment whose excitation properties may not be very diverse, the wide range of star-forming activity observed in the central regions of starburst galaxies seems to give rise to a wide range of physical properties of the associated warm molecular gas.

A good choice of a representative galaxy of the class of normal starburst galaxies is the prototypical Sy2 galaxy NGC 1068. Indeed, this galaxy has $L_{FIR} = 1.5 \times 10^{11}\ L_\odot$ (Planesas, Scoville, & Myers 1991) and high ^{12}CO (1–0) brightness temperatures ($T_b \sim 10$–15 K over linear sizes of ~ 200 pc; Planesas et al. 1991) in the inner 30″. In this region, intense star formation is taking place (Planesas et al. 1991 and references therein), and over the same area, it is $R_{10} = 14$ and $r_{12} = 1.1$ (Table 1). In this case, the parameter space of the LVG models that corresponds to LTE conditions [$n(H_2) \gtrsim 10^4$ cm^{-3}] with $T_{kin} \gtrsim 20$ K and $\tau(^{13}CO) = 0.07$ can account for these ratios within their reported errors.

In very IR-luminous mergers/interacting galaxies with high values of R_{10}, the average conditions of the molecular gas can be even more extreme, and in a few cases (see Aalto et al. 1995), the observed line ratios may imply the presence of a two-phase gas in the central starbursting regions of these galaxies. The galaxies NGC 5135 and Arp 220 in our sample have values of $R_{10} > 20$, but in our survey, only NGC 5135 is observed in both $J = 2$–1 and $J = 1$–0 for the ^{12}CO and ^{13}CO isotopes. The ultraluminous merger galaxy

Arp 220 has been studied by Aalto et al. (1995), where they use it as an extreme example to show that a single gas phase cannot account for the average $R_{10} = 10$–15, $r_{13} \approx 1.3$, and $r_{12} \approx 0.9$ line ratios found toward the centers of starburst galaxies.

We argue that Arp 220 is a special case of a starburst where a particularly low $r_{12} = 0.53$ and a possibly high $r_{13} > 1$ (Casoli et al. 1992) line ratio make it unlikely that a single gas phase can account for both (Aalto et al. 1995). However, this is not the case for the *average* values of R_{10}, r_{12}, and r_{13} observed in starburst nuclear regions where we find that a single gas phase can still reproduce these ratios fairly well. In order to examine the molecular gas properties of such systems in more detail, we conducted LVG modeling for three characteristic cases, namely, NGC 5135 and an "average" starburst for $R_{10} = 10$ and 15. For NGC 5135, we have assumed that the JCMT and the NRAO 12 m telescope sample approximately the same gas and therefore $r_{13} = 1.7$. The results are shown in Table 6.

In Table 6, it is shown that the line ratios of NGC 5135 as well as the ones of the "average" starburst can be reproduced fairly well by a single gas phase. Figure 8 illustrates the contour map of $\log \chi^2$ overlaid in the $[n(H_2), \Lambda]$ parameter space for NGC 5135.

In the case of Arp 220, we did not find a good fit for $r_{12} = 0.53$ and $r_{13} > 1$. Nevertheless, we must mention that this lower limit reported by Casoli et al. (1992) may not be reliable. We find $R_{21} = 18$ (see Table 3), which is in perfect agreement with their value. However, the value $r_{12} = 0.53$ deduced from our measurements and data taken from the literature (see Table 1) is lower than their reported value of $r_{12} = 0.7$. In order for $r_{13} > 1$, it has to be $R_{10} = (r_{13}/r_{12})R_{21} > 34$, which is plausible but has not been measured yet.

It is also interesting to note that for $r_{12} \approx 0.8$–1.0, the parameter space of $[T_{kin}, n(H_2), \Lambda]$ for which it is $R_{10} = 10$–15 and $1 < r_{13} \lesssim 1.5$ can be found within the regime of superthermally excited ^{13}CO $J = 1$–0 where $T_{ex}(1\text{–}0)/T_{kin} > 1$. This particular feature of the CO $J = 1$–0 transition has been noticed by Goldsmith (1972), de Jong et al. (1975), and Leung & Liszt (1976), and it occurs because collisional excitations from $J = 0$ to $J = 2$ occur at a comparable rate to those from $J = 0$ to $J = 1$, while spontaneous radiative decays are faster for $J = 2$–1 than for $J = 1$–0 ($A_{21}/A_{10} \approx 10$). As a result, the $J = 1$ level may become overpopulated. The effect tends to be quenched at high optical depths where radiative trapping sets in and thermalizes the levels. For this reason, it is the rare isotopes (e.g., ^{13}CO) that are expected to be superthermally excited not ^{12}CO. Generally, the conditions needed for the $J = 1$–0 line to be superthermal can be found in the regime where (1) $T_{kin} \gtrsim 20$ K, (2) $n(H_2) \gtrsim 2 \times 10^3$ cm^{-3}, and (3) $\tau \lesssim 0.1$ (Leung & Liszt 1976). Moreover, the larger the kinetic temperature of the clouds, the wider the density range over which superthermality of the $J = 1$–0 transition can occur; for example, for $T_{kin} = 60$ K, $\Lambda \sim 10^{-5}$ (km s^{-1} pc^{-1})$^{-1}$, this range is $n(H_2) \sim 10^3$–10^5 cm^{-3}. Such conditions are plausible for the average molecular gas clouds in the inner 1 kpc of a luminous starburst galaxy.

Thus, we conclude that the average line ratios $R_{10} = 10$–15, $r_{13} = 1.3$, and $r_{12} = 0.9$ found for the nuclear regions ($L \lesssim 1$ kpc) of Seyfert and/or starburst galaxies can be accounted for by a single, relatively warm ($T_{kin} \gtrsim 20$ K) gas phase. A two-component gas model, while obviously not excluded, becomes necessary only for $r_{12} \lesssim 0.6$. Probing the conditions in the star-forming circumnuclear regions of Seyfert and starburst galaxies in more detail requires estimates of additional line ratios like ^{12}CO, ^{13}CO (3–2)/(1–0). Multiple transitions of dense gas tracers like CS, HCN, and HCO+ can help separate the properties of any distinct gas phases that may be present in these regions. Finally, in order to avoid "averaging-in" colder molecular gas from the disk, all the aforementioned measurements have to be conducted at a high enough resolution that only the warm nuclear gas at $\lesssim 1$ kpc is sampled.

4.4. *Molecular Gas Mass Estimates for Warm and Cold Gas*

In principle, the presence of a global gradient of molecular gas properties can affect the global gas mass estimate $M(H_2)$ from the ^{12}CO $J = 1$–0 luminosity L_{CO} using the empirical standard Galactic conversion factor $X = M(H_2)/L_{CO} = 4.9\ M_\odot$ (K km s^{-1} pc^2)$^{-1}$ (Solomon & Barrett 1991). The reason is that X depends on the average H_2 density n and the brightness temperature T_b of the ^{12}CO $J = 1$–0 transition. For virialized molecular clouds and optically thick ^{12}CO emission, this dependency can be expressed simply as $X = 2.1\sqrt{n}/T_b$ (e.g., Maloney & Black 1988, but see also Bryant & Scoville 1996 for a recent detailed analysis), which, for Galactic molecular clouds, results in the aforementioned empirical value. From the LVG solutions for the warm gas in an average starburst galaxy (Table 6), we find that the use of the standard Galactic conversion factor may underestimate $M(H_2)$ by no more than a factor of ~ 3. Nevertheless, other factors like high-pressure confinement of the molecular clouds (e.g., Bryant & Scoville 1996) and heating by an enhanced cosmic-ray density (Allen 1996) may result in a more significant underestimate of gas mass.

The discrepancy can be more serious for cold and relatively dense gas. In the case of IC 5135, our LVG analysis indicates $X \approx 32$, and hence the standard Galactic conversion factor can underestimate the mass of the cold gas by a factor of ≈ 7. This factor could be even larger for lower kinetic temperatures (e.g., Allen & Lequeux 1993; Loinard, Allen, & Lequeux 1995) and lower metallicities associated with less processed gas in large galactocentric radii.

5. CONCLUSIONS

We have conducted a survey of the ^{12}CO, ^{13}CO $J = 1$–0, $J = 2$–1 lines for a sample of Seyfert galaxies in order to probe properties of their global molecular gas reservoir. The main conclusions of our study are as follows:

1. We find that the average value of the $\langle r_{12} \rangle = 0.71$ ratio for Seyfert galaxies as a class is smaller than the $\langle r_{12} \rangle = 0.9$ found for the centers of nearby spiral and starburst galaxies. A comparison of Seyfert galaxies with a large sample of galaxies with various degrees of nuclear activity like LINERs and starburst and quiescent spiral galaxies reveals that, especially in the case of Seyfert and starburst galaxies, there is a correlation between r_{12} and the ratio of the source size Ω_s to the beam size Ω_{mb}. In this correlation, it seems that the low r_{12} line ratios are associated with small values of Ω_s/Ω_{mb}.

2. This correlation could be due to the presence of a global gas excitation gradient where warm ($T_{kin} \gtrsim 20$ K) gas lies preferably in the central parts of the galaxy while a population of cold ($T_{kin} < 10$ K), optically thick molecular

clouds dominates the emission at large galactocentric distances. In Seyfert and starburst galaxies, the frequent presence of intense nuclear ($\lesssim 1$ kpc) star formation can readily establish such an excitation pattern.

3. We find that $\langle R_{10} \rangle = 12$ and $\langle R_{21} \rangle = 13$, irrespective of Seyfert type. These ratios are similar to the ones found for nearby spiral and starburst galaxies. High ($R > 15$) values are measured toward merging/interacting galaxies. We also find that low $R_{10} \lesssim 8$ ratios seem to be associated mainly with low values $r_{12} \lesssim 0.7$ that characterize a cold, optically thick and possibly subthermally excited gas phase that seems to dominate the extended CO emission. For this gas component, there are indications that the application of the standard Galactic conversion factor of CO luminosity to H_2 mass may significantly underestimate the amount of molecular gas present.

4. We used an LVG code to model the conditions of the molecular gas in a few specific examples of Seyfert galaxies whose CO emission was found to be dominated either by the cold and very likely extended gas component or by the warm nuclear gas. In the case of IC 5135, an IR-luminous Sy2/starburst galaxy, the gas over scales of ~ 6 kpc seems to be cold ($T_{\rm kin} < 10$ K) and subthermally excited, while in the inner 1 kpc of the archetypal Sy2/starburst galaxy, NGC 1068 is warmer ($T_{\rm kin} \gtrsim 20$ K). Moreover, we conclude that $R_{10} = 10$–15 and $1 < r_{13} \lesssim 1.5$ that are frequently measured toward the centers of Seyfert and starburst galaxies do not necessarily imply a two-component molecular cloud ensemble, as it has been proposed in previous studies, unless $r_{12} \lesssim 0.6$.

We would like to thank the superb crew of telescope operators at the NRAO 12 m telescope for their help in obtaining these observations, on many occasions under stressful conditions. We also thank the telescope operators at the James Clerk Maxwell Telescope for their assistance. We acknowledge Jessica Arlett for providing us with the fitting and plotting capabilities of the LVG code that we used to analyze our data, and the anonymous referee for useful comments. P. P. P. would like to thank William Wall for his critical reading of this work, and Hakon Dahle for his help with the interactive data language. Finally, we acknowledge the support of a research grant to E. R. S. from the Natural Sciences and Engineering Research Council of Canada.

This research has made use of the NASA/IPAC Extragalactic Database (NED), which is operated by the Jet Propulsion Laboratory, California Institute of Technology, under contract with the National Aeronautics and Space Administration.

APPENDIX

CONVOLUTION PROCEDURE FOR THE ^{12}CO (2–1) MEASUREMENTS

In order to estimate reliable ^{12}CO (2–1)/(1–0) line ratios with the NRAO 12 m telescope, we made observations of ^{12}CO (2–1) in a nine-point grid, centered on the point of the ^{12}CO (1–0) measurement. The HPBW of the NRAO 12 m telescope at 115 and 230 GHz is $\theta_1 = 55''$ and $\theta_2 = 32''$, respectively; the grid cell has dimensions of $\Delta\theta_c \approx \theta_2/2 \approx 15''$. This dense sampling is necessary for a reliable convolution of the ^{12}CO (2–1) to the resolution of the ^{12}CO (1–0) measurement and the subsequent estimate of their ratio.

The relation between the main-beam brightness temperatures $T_{\rm mb}^{(1)}(1\text{–}0)$ and $T_{\rm mb}^{(2)}(2\text{–}1)$ and the true brightness temperature distributions T_{10} and T_{21} of the ^{12}CO, $J = 1$–0 and $J = 2$–1 emission, respectively, can be expressed as follows:

$$T_{\rm mb}^{(1)}(1\text{–}0)(\xi, n) = \frac{1}{\Omega_{\rm mb}(1)} \int_{4\pi} P_1(\xi - \xi', n - n') T_{10}(\xi', n') d\xi'\, dn' \tag{A1}$$

and

$$T_{\rm mb}^{(2)}(2\text{–}1)(\xi, n) = \frac{1}{\Omega_{\rm mb}(2)} \int_{4\pi} P_2(\xi - \xi', n - n') T_{21}(\xi', n') d\xi'\, dn' \,, \tag{A2}$$

where P_1 and P_2 are the beam patterns of the NRAO 12 m telescope at 115 and 230 GHz, respectively, and $\Omega_{\rm mb}(1)$ and $\Omega_{\rm mb}(2)$ are their volume integrals [$\Omega_{\rm mb}(1) > \Omega_{\rm mb}(2)$]. A Gaussian is a good approximation of the telescope's main beam (Jewell 1990) for both ^{12}CO transitions; therefore, we can write

$$P_k(\xi, n) = \exp\left[-4 \ln 2 \left(\frac{\xi^2 + n^2}{\theta_k^2}\right)\right] \qquad \text{with} \qquad \Omega_{\rm mb}(k) = \frac{\pi}{4 \ln 2}\, \theta_k^2 \qquad k = 1, 2 \,. \tag{A3}$$

In order to estimate the (2–1)/(1–0) line ratio at the common resolution of the ^{12}CO (1–0) observation, we need to evaluate

$$T_{\rm mb}^{(1)}(2\text{–}1)(\xi, n) = \frac{1}{\Omega_{\rm mb}(1)} \int_{4\pi} P_1(\xi - \xi', n - n') T_{21}(\xi', n') d\xi'\, dn' \,. \tag{A4}$$

After substituting the expressions ($k = 1, 2$) from equation (A3) into equations (A2) and (A4) and taking their Fourier transform F and dividing, we obtain

$$F[T_{\rm mb}^{(1)}(2\text{–}1)] = F(D) F[T_{\rm mb}^{(2)}(2\text{–}1)] \,, \tag{A5}$$

where

$$D(\xi, n) = \frac{1}{\Omega_d} \exp\left[-4 \ln 2 \left(\frac{\xi^2 + n^2}{\theta_1^2 - \theta_2^2}\right)\right] \qquad \text{with} \qquad \Omega_d = \Omega_{\rm mb}(1) - \Omega_{\rm mb}(2) \tag{A6}$$

is the "differential" beam pattern. If we now apply the inverse Fourier transform in equation (A5) and substitute the expression from equation (A6), then for the central point $(\xi, n) = (0, 0)$, we get

$$T_{\rm mb}^{(1)}(2\text{–}1) = \int_{-\infty}^{+\infty}\int_{-\infty}^{+\infty} D(\xi, n) T_{\rm mb}^{(2)}(2\text{–}1)(\xi, n) d\xi\, dn\ . \tag{A7}$$

The main-beam brightness temperature $T_{\rm mb}^{(2)}(2\text{–}1)$ is sampled at only nine points within a radius $R \equiv \theta_1/2$. This nine-point grid provides dense enough sampling to recover all the spatial information needed to reconstruct $T_{\rm mb}^{(2)}(2\text{–}1)(\xi, n)$. Indeed, the beam pattern $P_2(\xi, n)$ can be seen as the response of a spatial filter that filters out any details "finer" than the resolution limit of the telescope, and from the Fourier transform of equation (A2), we get

$$F[T_{\rm mb}^{(2)}(2\text{–}1)] = \frac{1}{\Omega_{\rm mb}(2)} F(P_2) F(T_{21})\ , \tag{A8}$$

where

$$F(P_2) = \exp\left[-\frac{\theta_2^2}{16 \ln 2} (k_\xi^2 + k_n^2) \right]. \tag{A9}$$

According to the sampling theorem, the grid spacing $\Delta\theta_c = \theta_2/2$ corresponds to a spatial cutoff frequency of $k_c = \pi/\Delta\theta_c$. Substituting this frequency into $F(P_2)$, we find that, for each dimension, $F(P_2)(k_c, 0) = F(P_2)(0, k_c) = 0.028$. The smallness of this value guarantees that such a sampling is dense enough to recover most of the spatial frequency range of the $T_{\rm mb}^{(2)}(2\text{–}1)(\xi, n)$ distribution.

Application of the sampling theorem (Shannon 1949) for two dimensions gives the expression that interpolates $T_{\rm mb}^{(2)}(2\text{–}1)(\xi, n)$ from its discrete measurements, namely,

$$T_{\rm mb}^{(2)}(2\text{–}1)(\xi, n) = \sum_{\lambda_\xi}\sum_{\lambda_n} T_{\rm mb}^{(2)}(2\text{–}1)(\lambda_\xi \Delta\theta_c, \lambda_n \Delta\theta_c)\ \mathrm{sinc}\left[\frac{\pi}{\Delta\theta_c}(\xi - \lambda_\xi \Delta\theta_c)\right] \mathrm{sinc}\left[\frac{\pi}{\Delta\theta_c}(\xi - \lambda_n \Delta\theta_c)\right], \tag{A10}$$

where $(\lambda_\xi, \lambda_n) \in (-\infty, +\infty)$ defines the grid points. Substituting equation (A10) into equation (A7), and after some calculations, we finally get

$$T_{\rm mb}^{(1)}(2\text{–}1) = \sum_{\lambda_\xi}\sum_{\lambda_n} W(\lambda_\xi, \lambda_n) T_{\rm mb}^{(2)}(2\text{–}1)(\lambda_\xi \Delta\theta_c, \lambda_n \Delta\theta_c)\ , \tag{A11}$$

where the "weighting" factor $W(\lambda_\xi, \lambda_n)$ can be expressed in the form

$$W(\lambda_\xi, \lambda_n) = \left\{\int_0^1 \cos\,[\pi(\lambda_\xi x)] e^{-\rho^2 x^2} dx\right\}\left\{\int_0^1 \cos\,[\pi(\lambda_n x)] e^{-\rho^2 x^2} dx\right\}, \tag{A12}$$

with

$$\rho = \frac{\pi}{4\sqrt{\ln 2}} \frac{\sqrt{\theta_1^2 - \theta_2^2}}{\Delta\theta_c}\ . \tag{A13}$$

It can be shown that in the dense sampling case, where $\rho \gg 1$, $W(\lambda_\xi, \lambda_n)$ is normalized, as expected, namely,

$$\int_{-\infty}^{+\infty}\int_{-\infty}^{+\infty} W(\lambda_\xi, \lambda_n) d\lambda_\xi\, d\lambda_n = 1\ . \tag{A14}$$

We sampled the HPBW $= \theta_1$ in a grid of nine points, and from the nine weighting factors, only two are independent: $W(0, 0) = 0.100$ and $W(1, 0) = 0.073$. The rest of the weighting factors satisfy the relations: $W(1, 0) = W(0, 1) = W(-1, 0) = W(0, -1)$ and $W(1, 1) = W(-1, -1) = W(1, -1) = W(-1, 1) = W(1, 0)^2/W(0, 0)$. We have used equation (A11), together with the values of the weighting factors $W(\lambda_\xi, \lambda_n)$ estimated above, in order to produce the convolved spectrum $T_{\rm cn}[^{12}\mathrm{CO}\ (2\text{–}1)] = T_{\rm mb}^{(1)}(2\text{–}1)$ that we use to estimate the ^{12}CO (2–1)/(1–0) line ratio.

REFERENCES

Aalto, S. 1994, Ph.D. thesis, Chalmers Univ. Technol.
Aalto, S., Booth, R. S., Black, J. M., & Johansson, L. E. B. 1995, A&A, 300, 369
Allen, R. J. 1996, in New Extragalactic Perspectives in the New South Africa, ed, D. L. Block & J. M. Greenberg (Dordrecht: Kluwer), 50
Allen, R. J., Le Bourlot, J., Lequeux, J., Pineau des Forêts, G., & Roueff, E. 1995, ApJ, 444, 157
Allen, R. J., & Lequeux, J. 1993, ApJ, 410, L15
Alloin, D., Barvainis, R., Gordon, M. A., & Antonucci, R. R. J. 1992, A&A, 265, 429
Atherton, P. D., Reay, N. K., & Taylor, K. 1985, MNRAS, 216, 17P
Bally, J., Stark, A. A., Wilson, R. W., & Henkel, C. 1988, ApJ, 324, 223
Barvainis, R. 1993, ApJ, 412, 513
Barvainis, R., Alloin, D., & Antonucci, R. P. I. 1989, ApJ, 337, L69
Binney, J., Gerhard, O. E., Stark, A. A., Bally, J., & Uchida, K. I. 1991, MNRAS, 252, 210
Braine, J., & Combes, F. 1992, A&A, 264, 433
Braine, J., Combes, F., Casoli, F., Dupraz, C., Gerin, M., Klein, U., Wielebinski, R., & Brouillet, N. 1993, A&AS, 97, 887
Bryant, P. M., & Scoville, N. Z. 1996, ApJ, 457, 678
Casoli, F., Combes, C., Dupraz, C., Gerin, M., Encrenaz, P., & Salez, M. 1988, A&A, 192, L17

Casoli, F., Dupraz, C., & Combes, F. 1992, A&A, 264, 55
Chini, R., Kreysa, E., & Biermann, P. L. 1989, A&A, 219, 87
Chini, R., Krugel, E., & Steppe, H. 1992, A&A, 255, 87
de Jong, T., Chu, S., & Dalgarno, A. 1975, ApJ, 199, 69
de Vaucouleurs, G., de Vaucouleurs, A., Corwin, H. G., Jr., Buta, R. J., Paturel, G., & Fouqué, P. 1991, Third Reference Catalogue of Bright Galaxies (New York: Springer)
Devereux, N., Taniguchi, Y., Sanders, D. B., Nakai, N., & Young J. S. 1994, AJ, 107, 2006
Eckart, A., Cameron, M., Jackson, J. M., Genzel, R., Harris, A. I., Wild, W., & Zinnecker, H. 1991, ApJ, 372, 67
Eckart, A., van der Werf, P. P., Hofmann, A., & Harris, A. I. 1994, ApJ, 424, 627
Fuente, A., Martin-Pintado, J., Gernicharo, J., & Bachiller, R. 1993, A&A, 276, 473
Goldsmith, P. F. 1972, ApJ, 176, 597
Goldsmith, P. F., & Langer, W. D. 1978, ApJ, 222, 881
Gusten, R., Walmsley, C. M., Ungerechts, H., & Churchwell, E. 1985, A&A, 142, 381
Harris, A. I., Hills, R. E., Stutzki, J., Graf, U. U., Russel, A. P. G., & Genzel, R. 1991, ApJ, 382, L75
Heckman, T. M., Blitz, L., Wilson, A. S., Armus, L., & Miley, G. K. 1989, ApJ, 342, 735
Heckman T. M., et al. 1995, ApJ, 452, 549
Henkel, C., & Mauersberger, R. 1993, A&A, 274, 730
Jewell, P. 1990, User's Manual for the NRAO 12 m Millimeter-Wave Telescope (Tucson: NRAO)
Knapp, G. R., Phillips, T. G., Huggins, P. J., Leighton, R. B., & Wannier, P. G. 1980, ApJ, 240, 60
Krolik, J. H., & Begelman, M. C. 1986, ApJ, 308, L55
Kukula, M. J., Pedlar, A., Baum, S. A., & O' Dea, C. O. 1995, MNRAS, 276, 1262
Langer, W. D., & Penzias, A. A. 1993, ApJ, 408, 539
Leung, C. M., & Liszt, H. S. 1976, ApJ, 208, 732
Linden, S. V., Biermann, P. L., Duschl, W. J., Lesch, H., & Schmutzler, T. 1993, A&A, 280, 468
Loinard, L., Allen, R. J., & Lequeux, J. 1995, A&A, 301, 68
Maiolino, R., & Rieke, G. H. 1995, ApJ, 454, 95
Maiolino, R., Ruiz, M., Rieke, G. H., & Keller, L. D. 1995, ApJ, 446, 561
Maiolino, R., Ruiz, M., Rieke, G. H., & Papadopoulos, P. 1997, ApJ, 485, 552
Maloney, P., & Black, J. H. 1988, ApJ, 325, 389
Matthews, H. E. 1996, The James Clerk Maxwell Telescope: A Guide for the Prospective User (Hilo: JAC)
Meixner, M., Puchalsky, R., Blitz, L., Wright, M., & Heckman, T. 1990, ApJ, 354, 158
Morgan, W. W., & Dreiser, R. D. 1983, ApJ, 269, 438
Norman, C., & Scoville, N. 1988, ApJ, 332, 124
Papadopoulos, P. P., Seaquist, E. R., & Scoville, N. Z. 1996, ApJ, 465, 173
Planesas, P., Scoville, N. Z., & Myers, S. T. 1991, ApJ, 369, 364
Radford, S. J. E., Solomon, P. M., & Downes, D. 1991, ApJ, 368, L15
Richardson, K. J. 1985, Ph.D. thesis, Dept. Phys., Queen Mary College, Univ. London
Rieke, G. H., Lebofsky, M. J., Thompson, R. I., Low, F. J., & Tokunaga, A. T. 1980, ApJ, 238, 24
Rigopoulou, D., Lawrence, A., White, G. J., Rowan-Robinson, M., & Church, S. E. 1996, A&A, 305, 747
Sage, L. J., & Isbell, D. W. 1991, A&A, 247, 320
Sanders, D. B., Soifer, B. T., Elias, J. H., Madore, B. F., Matthews, K., Neugebauer, G., & Scoville, N. Z. 1988, ApJ, 325, 74
Scoville, N. Z., Sargent, A. I., Sanders, D. B., & Soifer, B. T. 1991, ApJ, 366, L5
Shannon, C. E. 1949, Proc. IRE, 37, 10
Shields, J. C., & Fillipenko, A. V. 1990, AJ, 100, 1034
Solomon, P. M., & Barrett, J. W. 1991, in IAU Symp. 146, Dynamics of Galaxies and Molecular Cloud Distribution, ed. F. Combes & F. Casoli (Dordrecht: Kluwer), 235
Spergel, D. N., & Blitz, L. 1992, Nature, 357, 665
Stark, A. A., Gerhard, O. E., Binney, J., & Bally, J. 1991, MNRAS, 248, 1P
Stephens, M. A. 1970, J. R. Statistical Soc., Ser. B, 32, 115
Telesco, C. M., Becklin, E. E., Wynn-Williams, C. G., & Harper, D. A. 1984, ApJ, 282, 427
Telesco, C. M., & Dreher, R. 1988, ApJ, 334, 573
Wall, W. F., & Jaffe, D. T. 1990, ApJ, 361, L45
Wall, W. F., Jaffe, D. T., Bash, F. N., Israel, F. P., Maloney P. R., & Baas, F. 1993, ApJ, 414, 98
Wall, W. F., Jaffe, D. T., Israel, F. P., & Bash, F. N. 1991, ApJ, 380, 384
Wild, W., Harris, A. I., Eckart, A., Genzel, R., Graf, U. U., Jackson, J. M., Russell, A. P. G., & Stutzki, J. 1992, A&A, 265, 447
Wilson, A. S., & Ulvestad, J. S. 1982, ApJ, 263, 576
Wynn-Williams, C. G., & Becklin, E. E. 1993, ApJ, 412, 535
Young, J. S., & Sanders, D. B. 1986, ApJ, 302, 680